

AD-780 731

POLARIZED RADIANCE. VOLUME II. POLAR-
IZED SPECTRAL EMITTANCE FROM 4 TO 14
MICROMETERS

J. R. Maxwell, et al

Environmental Research Institute of Michigan

Prepared for:

Ballistic Research Laboratories

May 1974

DISTRIBUTED BY:

NTIS

National Technical Information Service
U. S. DEPARTMENT OF COMMERCE
5285 Port Royal Road, Springfield Va. 22151

UNCLASSIFIED

SECURITY CLASSIFICATION OF THIS PAGE (When Data Entered)

AD-780731

REPORT DOCUMENTATION PAGE		READ INSTRUCTIONS BEFORE COMPLETING FORM
1. REPORT NUMBER CONTRACT REPORT NO. 155	2. GOVT ACCESSION NO.	3. RECIPIENT'S CATALOG NUMBER
4. TITLE (and Subtitle) POLARIZED RADIANCE (VOL.II): POLARIZED SPECTRAL EMITTANCE FROM 4 to 14 μ m		5. TYPE OF REPORT & PERIOD COVERED Final 10 April - 31 Dec 72
		6. PERFORMING ORG. REPORT NUMBER 192500-1-T(1) (Vol.II)
7. AUTHOR(s) J. R. Maxwell R. Vincent S. Weiner		8. CONTRACT OR GRANT NUMBER(s) DAAD05-72-C-0246
9. PERFORMING ORGANIZATION NAME AND ADDRESS Environmental Institute of Michigan P. O. Box 618 Ann Arbor, Michigan 48107		10. PROGRAM ELEMENT, PROJECT, TASK AREA & WORK UNIT NUMBERS 6.11.02B RDT&E 1T061102B11A
11. CONTROLLING OFFICE NAME AND ADDRESS USA Ballistic Research Laboratories Aberdeen Proving Ground, Maryland 21005		12. REPORT DATE MAY 1974
		13. NUMBER OF PAGES 67
14. MONITORING AGENCY NAME & ADDRESS (if different from Controlling Office)		15. SECURITY CLASS. (of this report) UNCLASSIFIED
		15a. DECLASSIFICATION/DOWNGRADING SCHEDULE
16. DISTRIBUTION STATEMENT (of this Report) Approved for public release; distribution unlimited.		
17. DISTRIBUTION STATEMENT (of the abstract entered in Block 20, if different from Report)		
18. SUPPLEMENTARY NOTES The work reported herein was conducted by the Environmental Research Institute of Michigan for the Ballistic Research Laboratories, Aberdeen Proving Ground, MD 21005 under Contract No. DAAD05-72-C-0246. Dr. Lawrence VandeKieft is Technical Monitor. Contracts and grants to the Institute for the support of sponsored research are administered through the Office of Contracts Administration.		
19. REPRODUCIBILITY STATEMENTS (Continue on reverse side if necessary) and identify by block number) Spectral Emittance Polarized Emittance Modeling		Reproduced by NATIONAL TECHNICAL INFORMATION SERVICE U S Department of Commerce Springfield VA 22151
20. ABSTRACT (Continue on reverse side if necessary and identify by block number) Volume II of this report provides the Ballistic Research Laboratories with a description of a model for predicting emission polarization from paints. The report includes a description of measurements that were made along with graphs of measurement data. Validation of the model shows that model predictions agree with measurement to within the measurement accuracy 70% of the time, thus allowing degree of polarization to be calculated for smooth-surfaced materials in the thermal IR region for any λ (from about 7 to 15 μ m) and any polar angle, with (Continued on reverse side)		

DD FORM 1 JAN 73 1473 EDITION OF 1 NOV 65 IS OBSOLETE

UNCLASSIFIED

SECURITY CLASSIFICATION OF THIS PAGE (When Data Entered)

UNCLASSIFIED

SECURITY CLASSIFICATION OF THIS PAGE(When Data Entered)

Block 20. Abstract

only a measurement of spectral emittance from 7 to 15 μ m at any near-normal incidence required.

A listing of model parameters appropriate to the sample paints supplied by BRL is included along with a document explaining the use of the computer programs and listings of the programs as well.

UNCLASSIFIED

SECURITY CLASSIFICATION OF THIS PAGE(When Data Entered)

FOREWORD

The work reported herein, covering the period 10 April 1972 to 31 December 1972, was carried out by the Infrared and Optics Division of the Environmental Research Institute of Michigan (formerly the Willow Run Laboratories of The University of Michigan), Ann Arbor, Michigan. The work was performed under Contract DAAD05-72-C-0216 for the Army Ballistic Research Laboratories, and was done in three parts, each of which represent one volume.

The three volumes are:

- I - Polarized Bidirectional Reflectance With Lambertian or Non-Lambertian Diffuse Component.
- II - Polarized Spectral Emittance From 4 to 14 μm .
- III - Wavelength Dependence of Polarized Bidirectional Reflectance.

The internal number for volume II of this report is 192500-1-T(II)

TABLE OF CONTENTS

FOREWORD.....	3
TABLE OF CONTENTS.....	5
LIST OF FIGURES.....	6
LIST OF TABLES.....	7
1. INTRODUCTION.....	8
2. MODEL DESCRIPTION.....	8
3. MEASUREMENTS.....	11
3.1. Instrument.....	11
3.2. Spectral Emittance.....	14
3.3. Polarized Emittance vs. Angle.....	19
4. MODEL VALIDATION.....	32
5. CONCLUSIONS.....	42
APPENDIX A: DETERMINATION OF EXPERIMENTAL ERROR IN MEASUREMENTS OF DEGREE OF POLARIZATION.....	43
APPENDIX B: DOCUMENTATION FOR CLASSICAL OSCILLATOR FITTING PROGRAM.....	45
APPENDIX C: DOCUMENTATION FOR PROGRAM 'EMISPOL'.....	49
APPENDIX D: PROGRAM LISTING - OSCILLATOR.....	51
APPENDIX E: PROGRAM LISTING - EMISPOL.....	55
APPENDIX F: PROGRAM LISTING AND INSTRUCTIONS FOR IBM SCIENTIFIC SUBROUTINE - FMFP.....	57
REFERENCES.....	67
DISTRIBUTION LIST.....	69

LIST OF FIGURES

1.	Schematic of FISR Fore-Optics.....	12
2.	Spectral Directional Emittance - A0-2017.....	16
3.	Spectral Directional Emittance - A0-2022.....	17
4.	Spectral Directional Emittance - A0-2023.....	18
5.	Relative Polarized Emittance vs. Polar Angle A0-2017 $\lambda = 9.3\mu\text{m}$	20
6.	Relative Polarized Emittance vs. Polar Angle A0-2017 $\lambda = 10.6\mu\text{m}$	21
7.	Relative Polarized Emittance vs. Polar Angle A0-2022 $\lambda = 5.3\mu\text{m}$	22
8.	Relative Polarized Emittance vs. Polar Angle A0-2022 $\lambda = 8.3\mu\text{m}$	23
9.	Relative Polarized Emittance vs. Polar Angle A0-2022 $\lambda = 9.7\mu\text{m}$	24
10.	Relative Polarized Emittance vs. Polar Angle A0-2022 $\lambda = 10.6\mu\text{m}$	25
11.	Relative Polarized Emittance vs. Polar Angle A0-2022 $\lambda = 12.0\mu\text{m}$	26
12.	Relative Polarized Emittance vs. Polar Angle A0-2023 $\lambda = 5.3\mu\text{m}$	27
13.	Relative Polarized Emittance vs. Polar Angle A0-2023 $\lambda = 8.3\mu\text{m}$	28
14.	Relative Polarized Emittance vs. Polar Angle A0-2023 $\lambda = 9.7\mu\text{m}$	29
15.	Relative Polarized Emittance vs. Polar Angle A0-2023 $\lambda = 10.6\mu\text{m}$	30
16.	Relative Polarized Emittance vs. Polar Angle A0-2023 $\lambda = 12.0\mu\text{m}$	31
17.	Theoretical Degree of Polarization and Normal Emissivity vs. Wavelength for O.D. Paint (Sample A01792).....	33
18.	Model-Measurement Comparison Relative Polarized Emittance vs. Polar Angle A0-2017 $\lambda = 10.6\mu\text{m}$	39
19.	Model-Measurement Comparison Relative Polarized Emittance vs. Polar Angle A0-2022 $\lambda = 10.6\mu\text{m}$	40
20.	Model-Measurement Comparison Relative Polarized Emittance vs. Polar Angle A0-2023 $\lambda = 10.6\mu\text{m}$	41

LIST OF TABLES

1.	Polarization Field Measurements.....	34
2.	Comparison of Theoretically Calculated and Experimentally Measured Degree of Polarization for Emittance for $\lambda = 9.83\mu\text{m}$ (O.D. Paint A01792).....	37
3.	Comparison of Theoretically Calculated and Experimentally Measured Degree of Polarization for O.D. Paints.....	38

1. INTRODUCTION

Most materials on the earth's surface emit a large portion of their radiated energy in the thermal-infrared wavelength region. If irregularities of the surface of a natural target are very large compared to the wavelength of emitted radiation, total emissivity measurements are the prime source of information. However, if the surface irregularities of a target are small compared to the wavelength of emitted radiation, the surface tends to be more specular and the electric vectors of this emitted radiation will vibrate in preferential directions, giving rise to an observable emission polarization. For relatively smooth surfaces, therefore, polarization measurements are an additional source of information. Since the surfaces of military targets are generally smoother and have more ordered geometric patterns than naturally occurring materials, polarization is a potentially important parameter for target discrimination.

The purpose of this report is to describe a phenomenological model for predicting emission polarization of paints using as input only a single, near-normal reflectivity spectrum.

2. MODEL DESCRIPTION

For the case of an emitting polished surface, that portion of the emitted radiance at some angle θ to the target surface normal that has its electric vector vibrating perpendicular to the plane of emission (containing the surface normal and the propagation vector), divided by half the radiance emitted by a blackbody at the same temperature, is called the perpendicular component $E_{\perp}(\theta)$ of the emissivity. [Note: All the emissivity components are wavelength dependent, but the λ notation will be suppressed.] Likewise, the parallel emissivity component $E_{\parallel}(\theta)$ defines that portion of radiation emitted with electric vector vibration parallel to the plane of emission. The total emissivity $E(\theta)$ is half the sum of $E_{\perp}(\theta)$ and $E_{\parallel}(\theta)$.

The degree of polarization for emission can be defined as:

$$P_E = [E_{\parallel}(\theta) - E_{\perp}(\theta)]/[E_{\parallel}(\theta) + E_{\perp}(\theta)]. \quad (1)$$

The relationship between the emission polarization components and reflection polarization components can be found from a consideration of the reflection experiment where source (at θ_i) and observed (at θ_r) are located on opposite sides of the target surface normal at an angle $\theta = \theta_i = \theta_r$. Let R_{\perp} and R_{\parallel} be the reflectivity components for radiation with electric vectors vibrating perpendicular and parallel, respectively, to the plane of incidence containing the incident and reflected rays. With the constraint that $\theta = \theta_i = \theta_r$, implying that the plane of emission coincides with the plane of incidence, Kirchhoff's law dictates (for equilibrium conditions) that

$$E(\theta)_{\perp} = 1 - R(\theta)_{\perp}, \quad (2a) \quad E(\theta)_{\parallel} = 1 - R(\theta)_{\parallel}. \quad (2b)$$

The reflectivity flux components are functions only of $\theta_i = \theta_r = \theta$, and the complex index of refraction of the target material is given by $N = n - ik$. Expressions for R_{\perp} and R_{\parallel} in terms of θ , n , and k are as follows [1]:

$$R_{\perp}(\theta) = \frac{[(a - \cos \theta)^2 + b^2]}{[(a + \cos \theta)^2 + b^2]} \quad (3a)$$

$$R_{\parallel}(\theta) = \left\{ \frac{[(a - \cos \theta)^2 + b^2]}{[(a + \cos \theta)^2 + b^2]} \right\} \times \left\{ \frac{[(a - \sin \theta \tan \theta)^2 + b^2]}{[(a + \sin \theta \tan \theta)^2 + b^2]} \right\}, \quad (3b)$$

where

$$a^2 = \frac{1}{2} \{n^2 - k^2 - \sin^2 \theta + [4n^2 k^2 + (n^2 - k^2 - \sin^2 \theta)^2]^{\frac{1}{2}}\}$$

and

$$b^2 = \frac{1}{2} \{-n^2 + k^2 + \sin^2 \theta + [4n^2 k^2 + (n^2 - k^2 - \sin^2 \theta)^2]^{\frac{1}{2}}\}$$

From Eqs. (1), (2), and (3), therefore, it is possible to express the degree of emission polarization P_E as a function of θ , n , and k .

For materials which exhibit reststrahlen bands in the thermal-IR wavelength region, n and k are strongly wavelength-dependent in that region. The wavelength dependence of P_E for a given material can be calculated from Eqs. (1), (2), and (3) if the dispersion curves of n and k are known. Once these dispersion curves have been determined as continuous functions of wavelength for a given paint, it is then possible to calculate the emission polarization for all θ as a function of λ . This will be calculated for several O.D. paints.

One means for determining the indices of refraction is the classical oscillator fitting method. The complex index of refraction $N = n - ik$ can be calculated as a function of frequency ν , according to a classical oscillator model of crystals [2], from the following equations:

$$2nk = \sum_j 4\pi p_j \nu_j^2 \left[\frac{\gamma_j \nu_j \nu}{(\nu_j^2 - \nu^2)^2 + \gamma_j^2 \nu_j^2 \nu^2} \right],$$

$$n^2 - k^2 = \epsilon_\infty + \sum_j 4\pi p_j \nu_j^2 \left[\frac{\nu_j^2 - \nu^2}{(\nu_j^2 - \nu^2)^2 + \gamma_j^2 \nu_j^2 \nu^2} \right], \quad (4)$$

where p_j , γ_j , and ν_j are the strength, width, and frequency, respectively, of the j^{th} lattice oscillator and ϵ_∞ is the high frequency dielectric constant. If these oscillator parameters are known, n and k are calculable from Eq. (4). If they are unknown, they can be estimated by the following procedure. Initial guesses for the oscillator parameters are assumed, (see Appendix D) and a normal incidence Fresnel reflectivity curve $R(\nu)$ is calculated from the equation:

$$R(\nu) = \left\{ \frac{[n(\nu) - 1]^2 + k^2(\nu)}{[n(\nu) + 1]^2 + k^2(\nu)} \right\} \quad (5)$$

A computer program, which employs an IBM scientific subroutine, [see Appendix F] compares the theoretical reflectivity curve calculated from Eq. (5) with an experimental normal incidence spectral reflectivity curve for a smooth surface of the specimen, changes the oscillator parameters in Eq. (4), calculates a new theoretical curve, and reiterates until a good fit is made between theoretical and experimental curves. With the oscillator parameters of the best-fitting theoretical curve, the indices can then be calculated from Eq. (4). (See Appendix D for use of Oscillator Program.)

3. MEASUREMENTS

The measurements in this program consisted of two phases. The first phase consisted of a spectral scan of the emittance from each sample with a normal angle of observation. The second phase consisted of angular scans of the emittance with receiver polarizer set alternately perpendicular and parallel to the receiver incidence plane. In this latter case, each scan took place at a particular wavelength.

In the following paragraphs we provide a brief description of the instrument which was used for these measurements, followed by data which resulted.

3.1 The Instrument

The field infrared spectroradiometer (FISR) which was utilized is a double-beam instrument with output proportional to the radiance difference between the objects filling the fields of the two Herschelian reflecting telescopes. The measurement of the difference is accomplished by a reflective chopper which alternately samples the radiation from the two telescopes. After being chopped, the radiation from the two telescopes is imaged at a common focal plane at which a field stop slit is placed, limiting the FOV to a $0.6' \times 2.5^\circ$ field. The fore-optics just described are illustrated in Figure 1. The chopped energy passing through the field stop slit is refocused, by a 90° off-axis ellipsoid mirror, onto an entrance aperture which lies immediately in front of the circular variable-filter (CVF) monochromator.

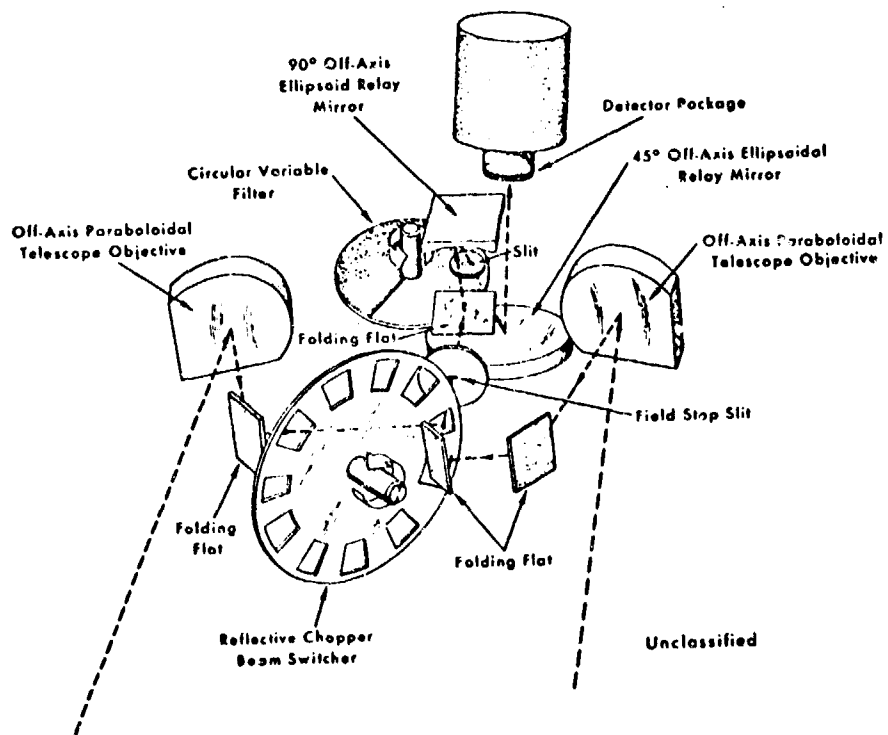


Figure 1. SCHEMATIC OF FIR FORE-OPTICS

The CVF then transmits a narrow spectral band of this energy to a 45° off-axis ellipsoid mirror, which refocuses it onto the detector.

The generated ac detector signal is amplified and then synchronously demodulated. The synchronous demodulator transforms those components of the signal which have the particular frequency of the chopper modulation into a proportional dc signal, while rejecting those components with different frequency (i.e., noise). Thus, at the output a dc signal is presented which has a value at any point in time proportional to the energy difference between the two optical beams at a particular wavelength determined by the CVF position. Mechanical rotation of the CVF provides a spectral scan. The output voltage is recorded by using a digital voltmeter as an analog-to-digital converter and printing on a digital paper-tape printer, and the wavelength is registered simultaneously by printing the digital output of a shaft encoder mechanically linked to the CVF.

The spectrometer portion of the system utilized a circular variable filter for spectral dispersion in the range from 2.5 to 14.5 μ m. The CVF has the advantage of providing more efficient energy transmission than a prism disperser, allowing faster spectral scan rates or narrower spectral resolution for a given energy input.

In order to achieve high system sensitivity, an indium antimonide and a mercury doped germanium detector are used to cover the wavelength regions 2.5 to 5.5 μ m and 4.5 to 14.5 μ m, respectively. These detectors are readily interchangeable, so one may be replaced by the other during the course of scanning from 2.5 to 14.5 μ m without stopping the instrument.

Two temperature-controlled blackbody calibration sources are provided for insertion at the entrance optics in either or both of the two channels. In the normal mode of operation, a blackbody remains in one channel, and the other channel, having previously been calibrated, views the target of interest. In this way the system can be used to measure absolute radiance. Alternatively, if the target temperature is known, or if a black surface at the same temperature is available, the spectral emittance of the surface can be determined. These blackbodies are only suitable for the spectral

range 4.5 to 14.5 μ m. Calibration sources below 4.5 μ m have not as yet been implemented. However, for these reflective wavelengths (less than 4.5 μ m), a calibrated reflectance panel may be inserted in the reference beam and the instrument then used to make relative reflectance measurements.

Supplementary instrumentation has been developed to permit the basic FISR equipment to be used for obtaining directional polarized emissivity data. Two similar samples maintained at different known temperatures are separately viewed through each port of the FISR, and the difference in radiance values is measured. From this measured difference, with the available temperature information, the emissivity can be calculated. The sample temperatures are maintained by thermally controlled water baths. The sample holder is designed to be operated either at a fixed viewing angle or by revolving and permitting a scan of the sample surface.

Complete details of the FISR can be found in reference 4.

3.2 Spectral Emittance

Figures 2, 3 and 4 show the spectral emittance data in plotted form. In each case there are many scans, some of which cover different spectral regions than others. Each scan number has its own symbol so it can be roughly identified on the plot. Shown also are curves representing both accuracy and precision of the measurements. Accuracy is determined with respect to both systematic and random errors. Precision is determined with respect to noise in the recorded voltage. (Reference 4 provides a complete discussion of determination of accuracy and precision in this context.)

Note that for all three samples, there is an apparent dip in the spectrum between 9.5 μ m and 10 μ m. This dip is interpreted to be a reststrahlen band. Structure of this sort arises from the wavelength dependence of the indices of refraction. (In section 1, we have described how one calculates the indices of refraction by use of a classical oscillator fitting method.)

Note also that in Figure 3 there is an apparent discrepancy in that scans numbers 3 and 4 are translated upward with respect to scans 2 and 23. This discrepancy appears to be due to a combination of calibration error and difficulty of maintaining accurate measurement of environment temperature during the measurements. The problem is still being analyzed. In the validation (see Section 4) scans 3 and 4 were used. In view of the apparent difficulty it is not clear that these were the most appropriate.

SPECTRAL DIRECTIONAL EMITTANCE

AO-2017

EMITTANCE	SYMBOL	RUN NO.	SCAN NO.
—	♦	146	2
---	x	146	3
----	•	146	9
	♦	146	10
	•	146	12
	•	146	14
	•	146	15
	•	146	17
	•	146	18
	•	146	20

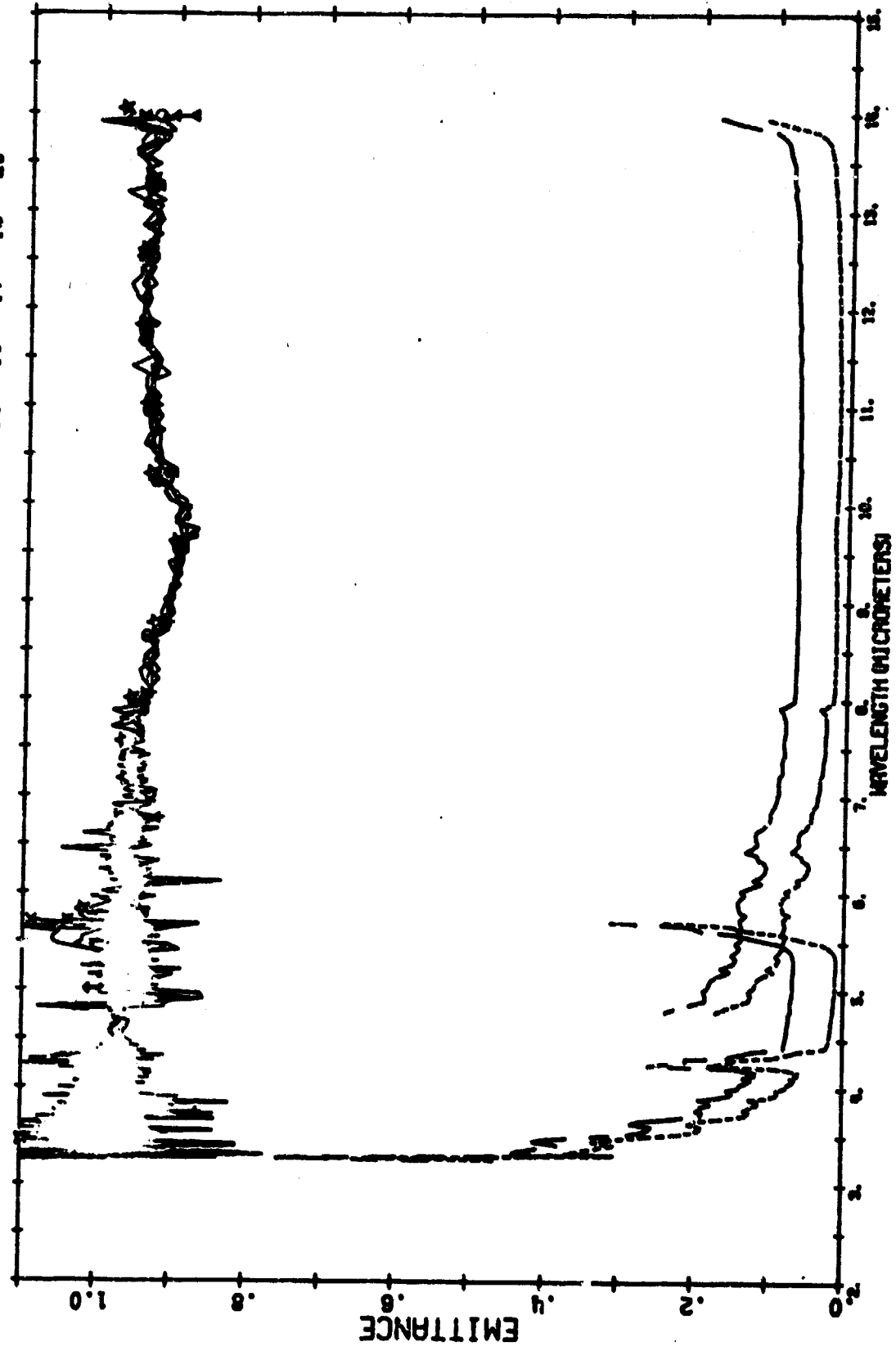


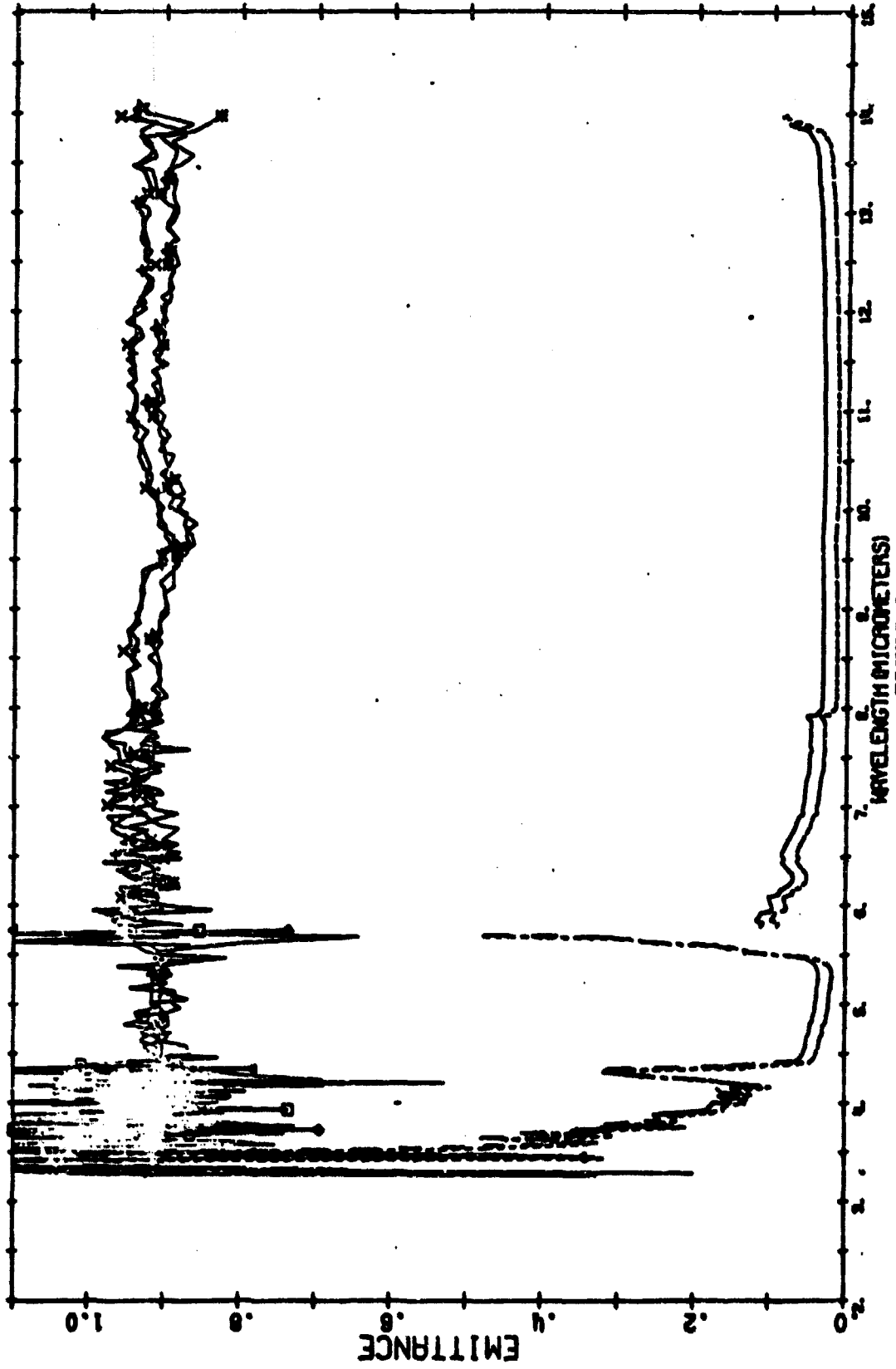
FIGURE 2

SPECTRAL DIRECTIONAL EMITTANCE

A0-2022

EMITTANCE
--- ACCURACY
- - - - - PRECISION

SYMBOL
RUN NO. 149 149 149 149 149 149 149 149 149
SCRN NO. 2 3 4 14 15 16 20 23



WAVELENGTH (MICROMETERS)
FIGURE 3

SPECTRAL DIRECTIONAL EMITTANCE

EMITTANCE
 ACCURACY
 PRECISION

AD-2023

SYMBOL
 RUN NO.
 SCAN NO.

148 148 148 148 148 148 148 148 148 148
 2 3 4 7 8 11 15 9

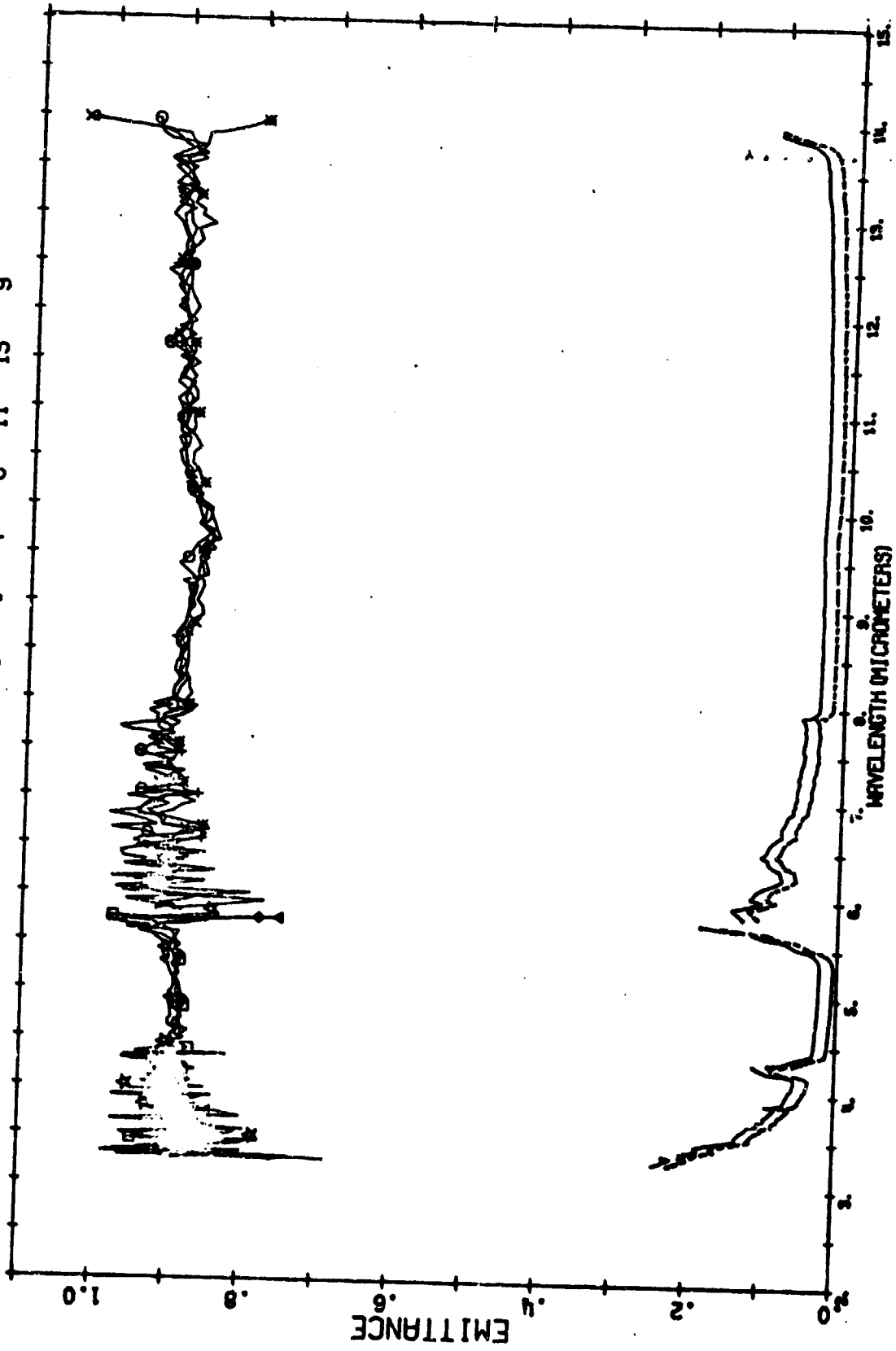


FIGURE 4

3.3 Polarized Emittance vs. Angle

Figures 5 through 16 show the variation for each sample at a variety of wavelengths of relative polarized emittance. In each case the curve

which represents parallel polarization is a plot of $e_{||}(\theta) = \frac{E_{||}(\theta)}{E_{||}(0)}$ and

that which represents perpendicular polarization is $e_{\perp}(\theta) = \frac{E_{\perp}(\theta)}{E_{\perp}(0)}$.

Therefore, for each angle, degree of polarization is extracted from the data by equation (1), where substituting $e_{||}(\theta)$ and $e_{\perp}(\theta)$ for $E_{\perp}(\theta)$ and $E_{||}(\theta)$ leaves P_E unchanged, since $E_{||}(0) = E_{\perp}(0) = E(0)$. [See Appendix A]. Comparison of model predictions with selected measurement data from this group is described in Section 4.

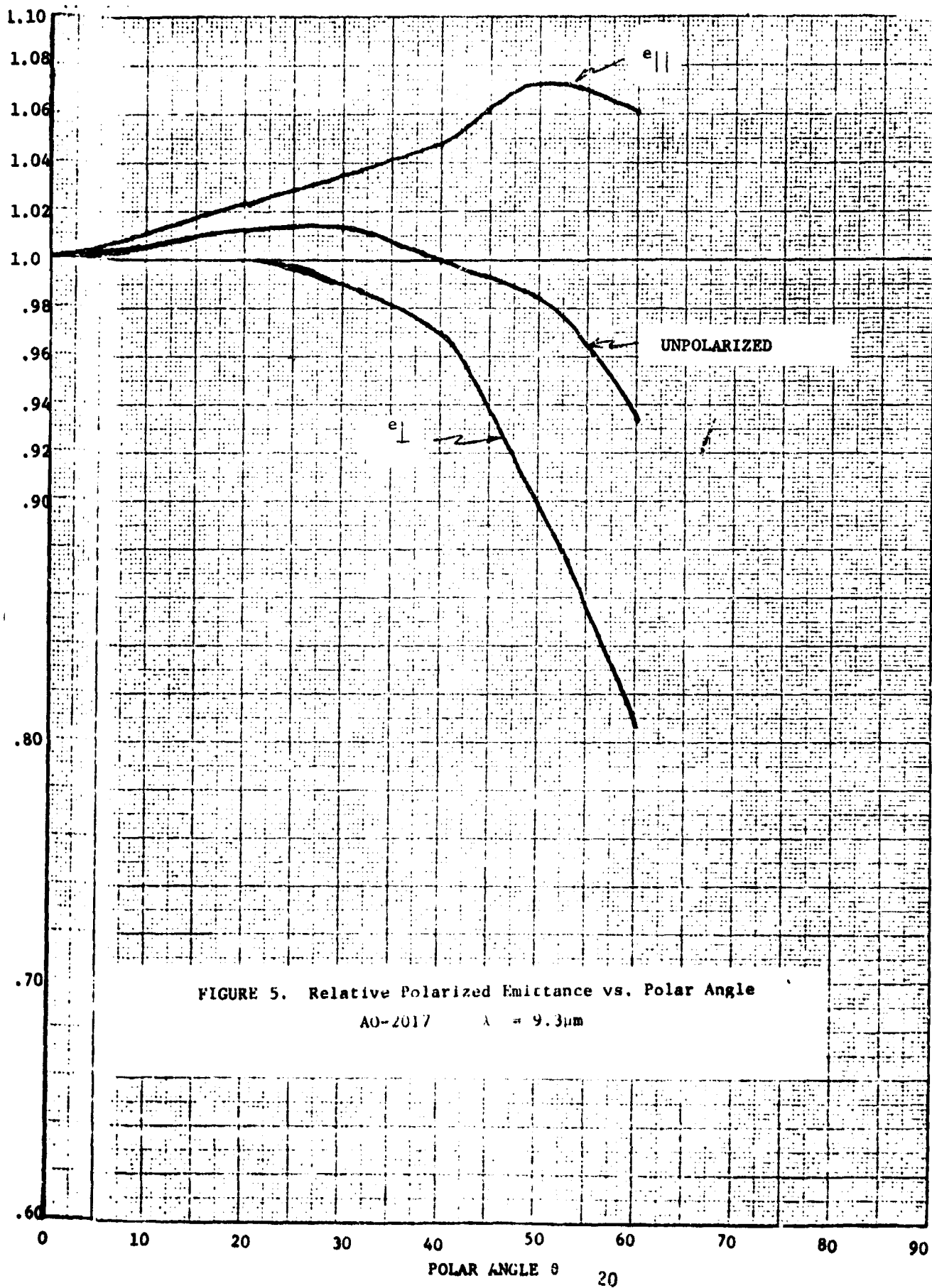


FIGURE 5. Relative Polarized Emittance vs. Polar Angle

AO-2017 $\lambda = 9.3 \mu\text{m}$

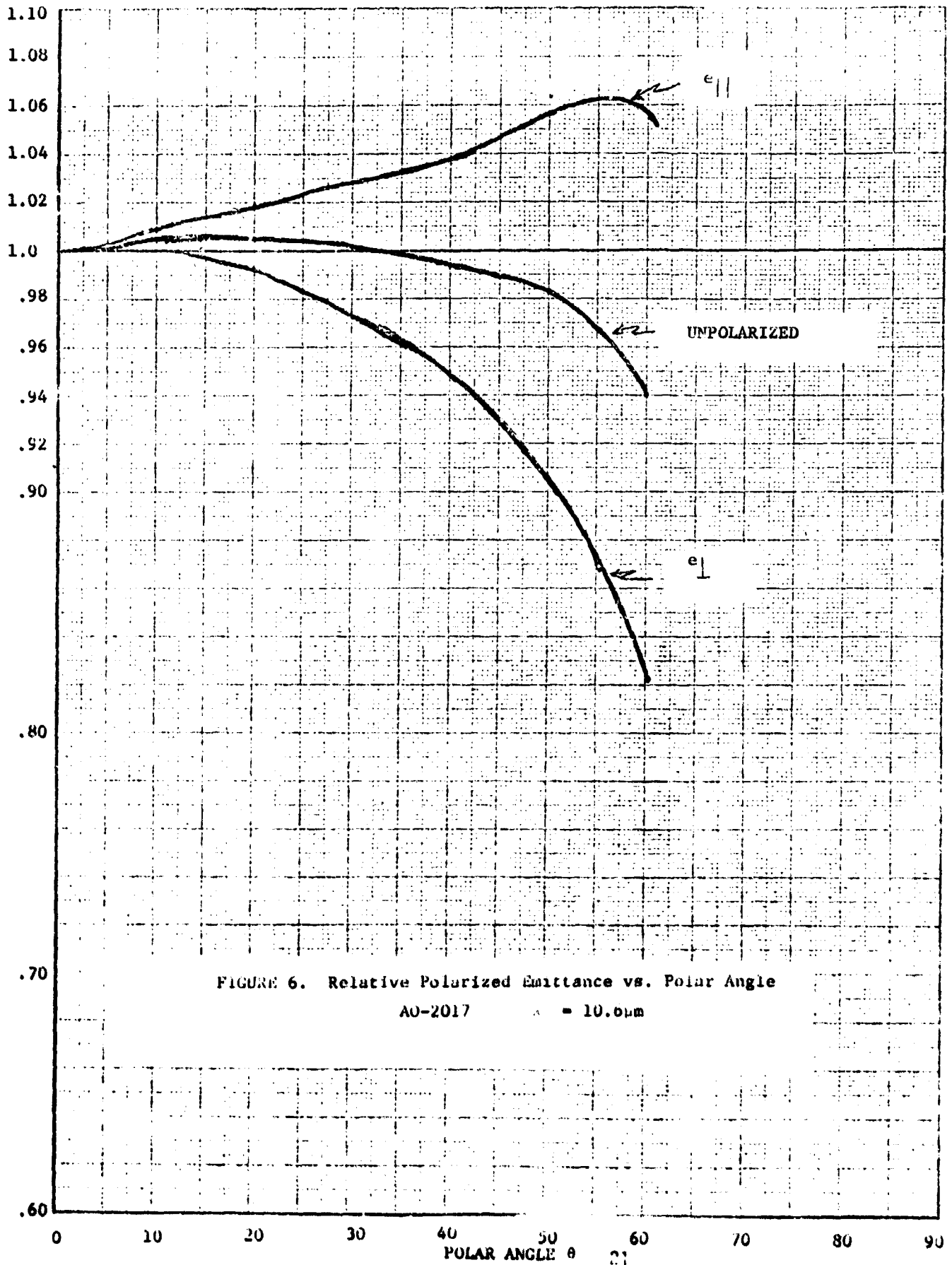


FIGURE 6. Relative Polarized Emittance vs. Polar Angle
 AO-2017 $\lambda = 10.6\mu\text{m}$

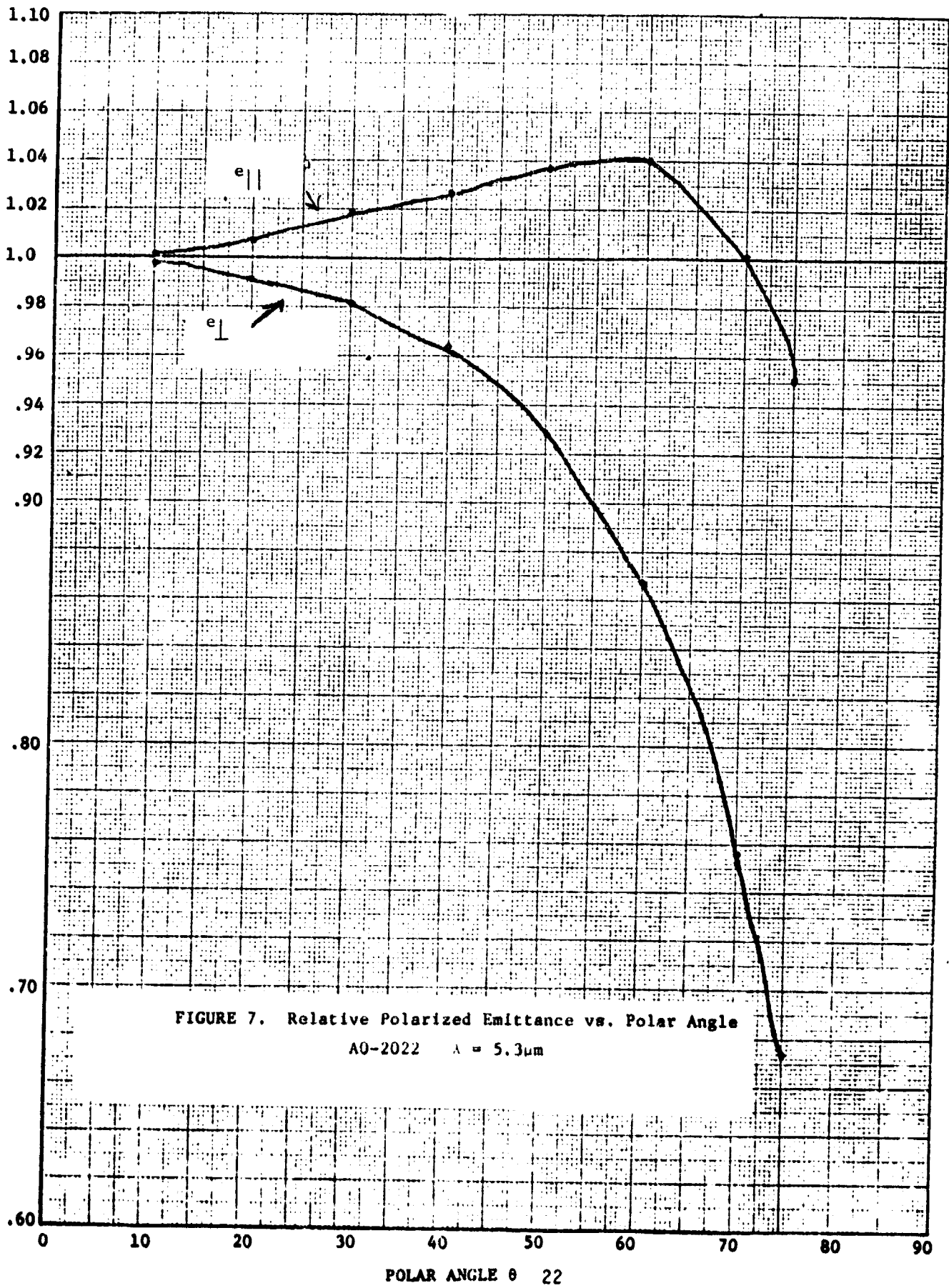
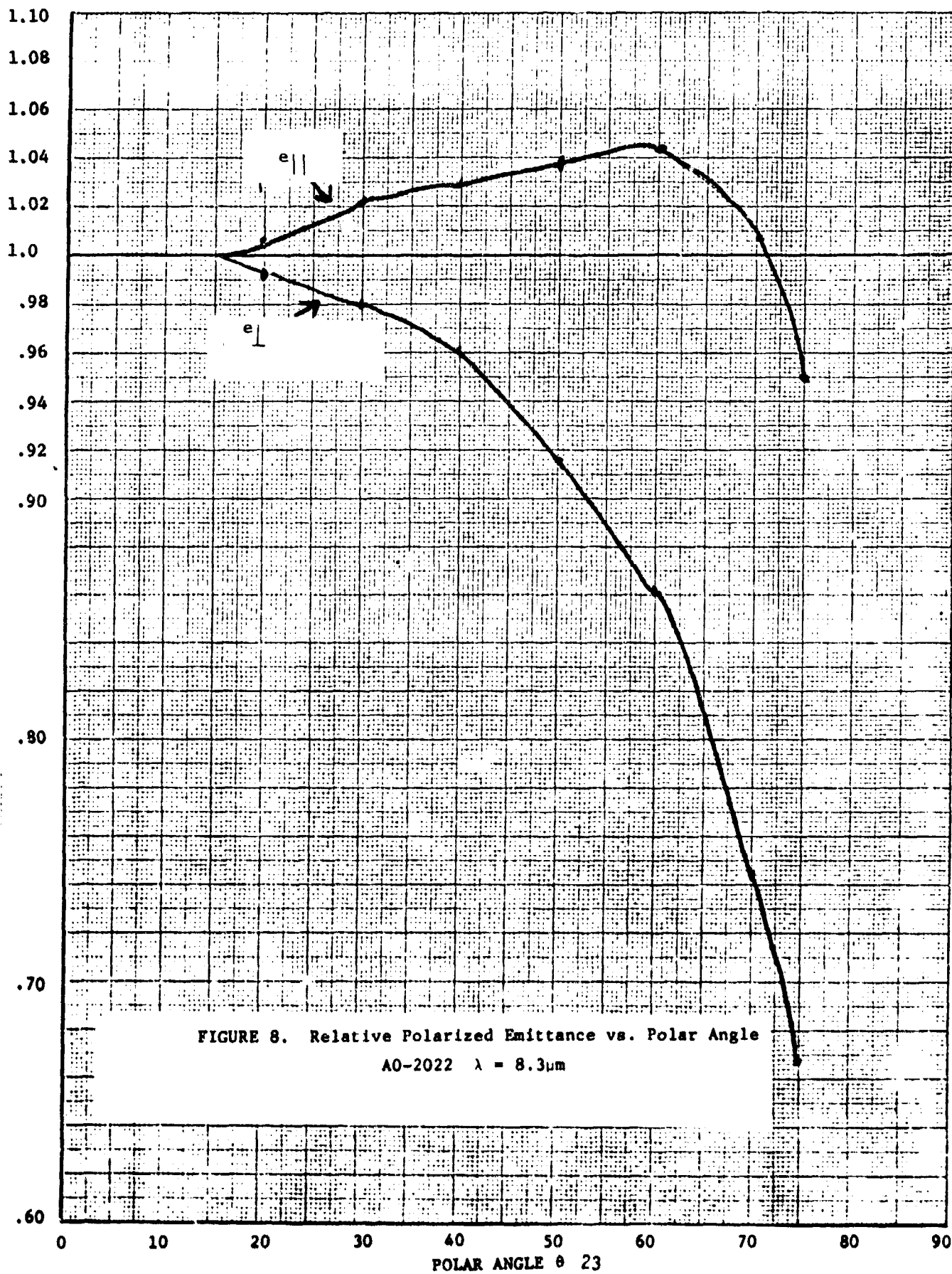


FIGURE 7. Relative Polarized Emittance vs. Polar Angle

A0-2022 $\lambda = 5.3\mu\text{m}$



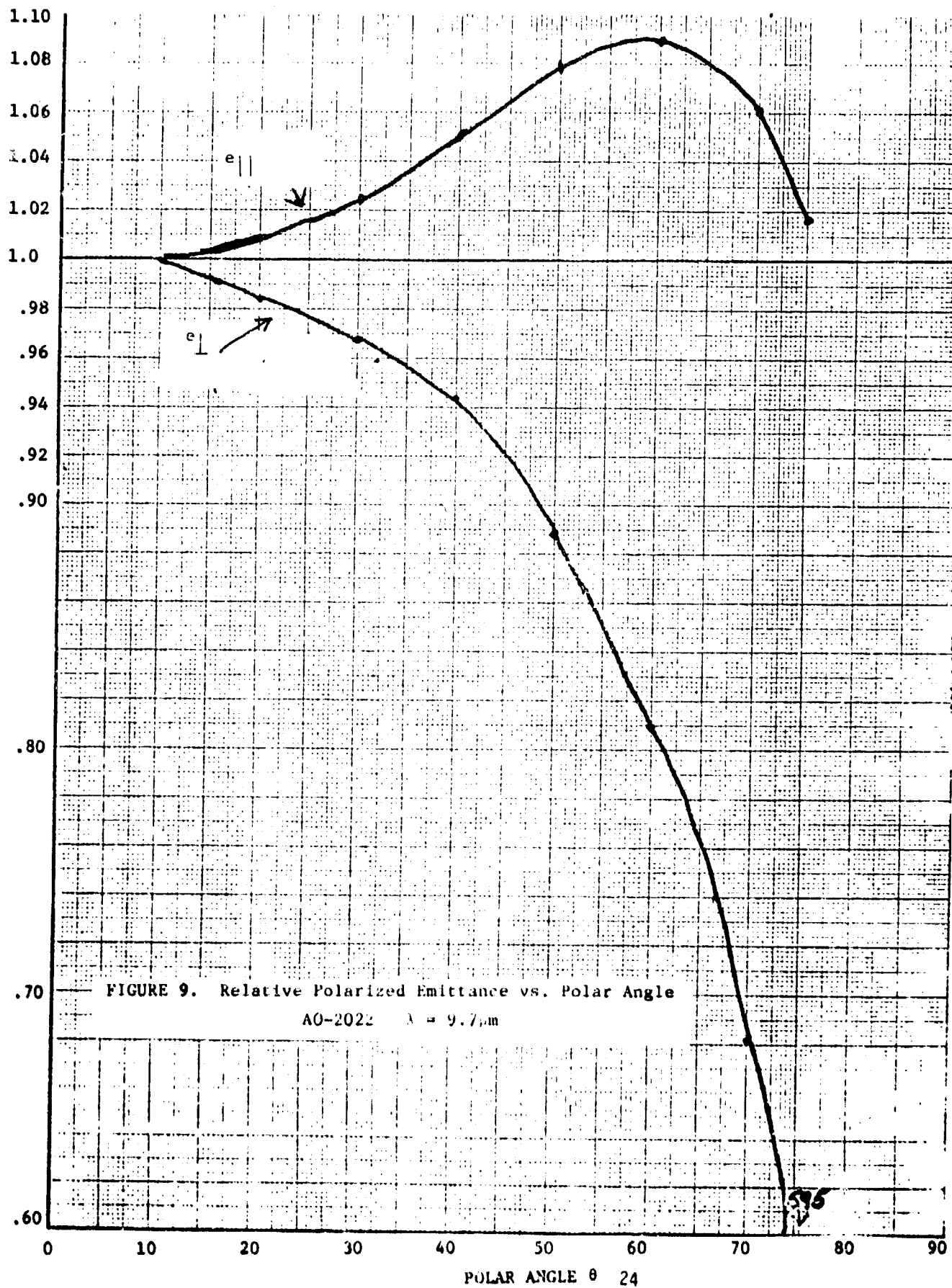


FIGURE 9. Relative Polarized Emittance vs. Polar Angle
 AO-2022 $\lambda = 9.7 \mu\text{m}$

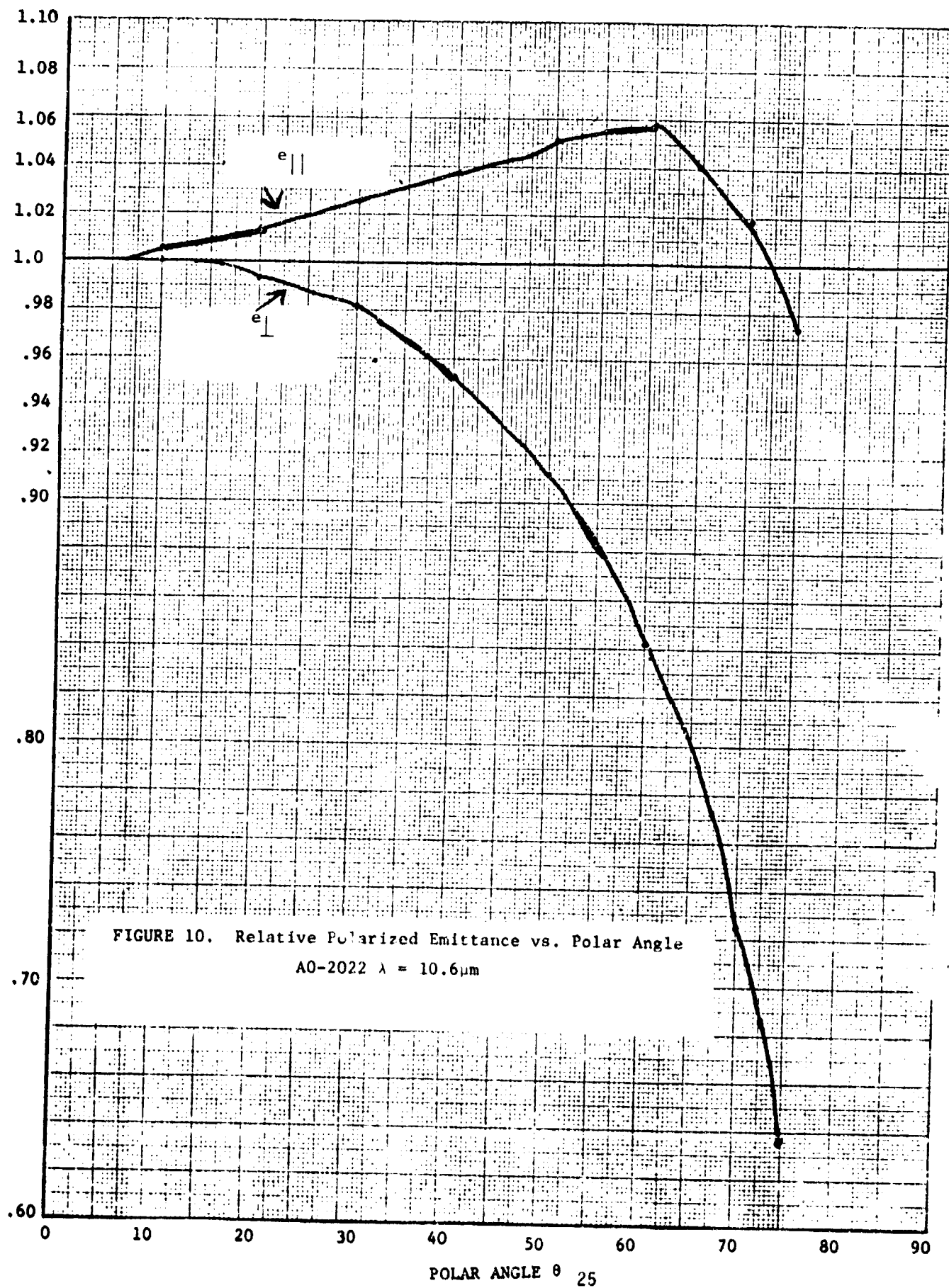


FIGURE 10. Relative Polarized Emittance vs. Polar Angle
 A0-2022 $\lambda = 10.6\mu\text{m}$

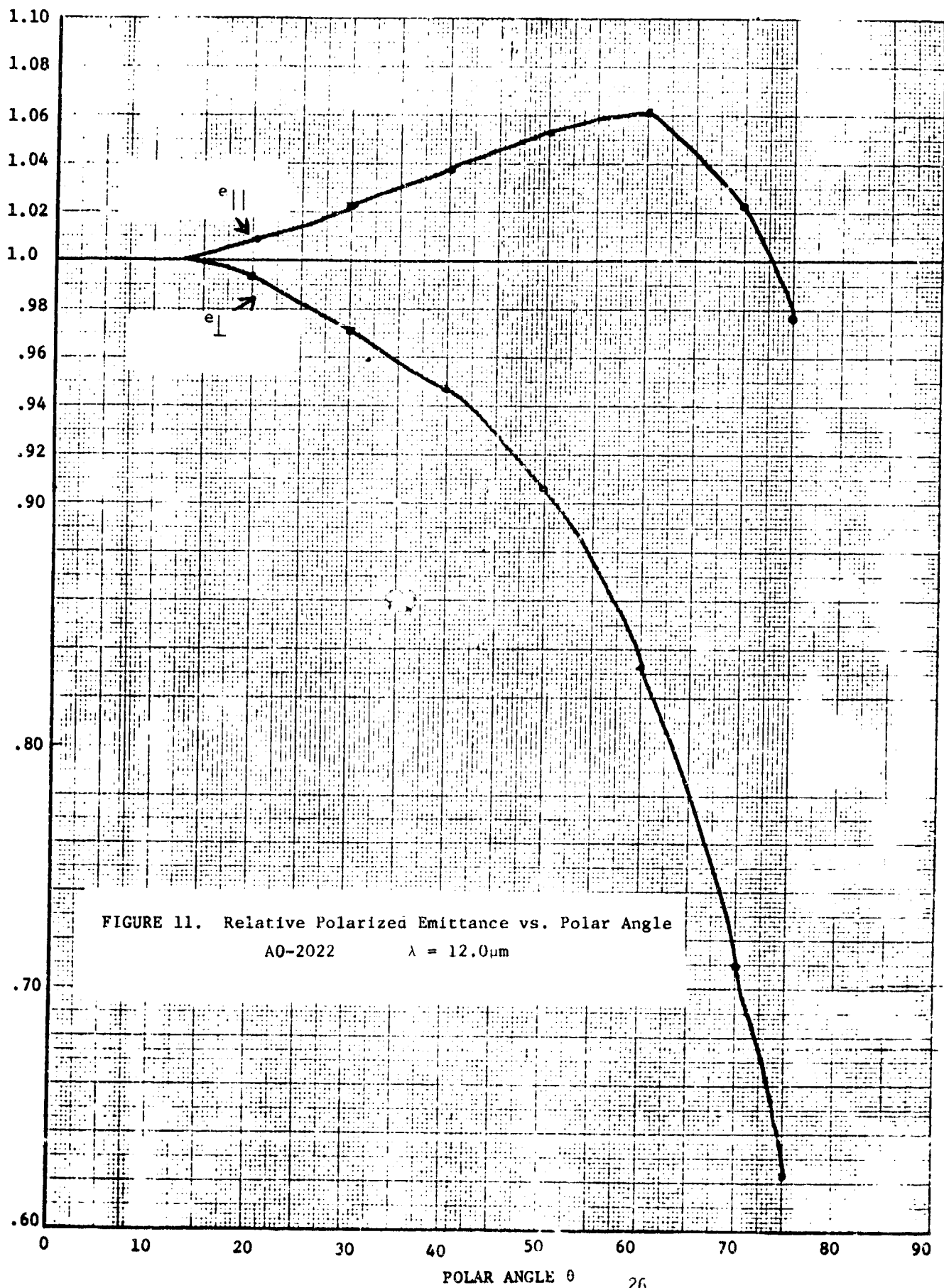


FIGURE 11. Relative Polarized Emittance vs. Polar Angle
 AO-2022 $\lambda = 12.0 \mu\text{m}$

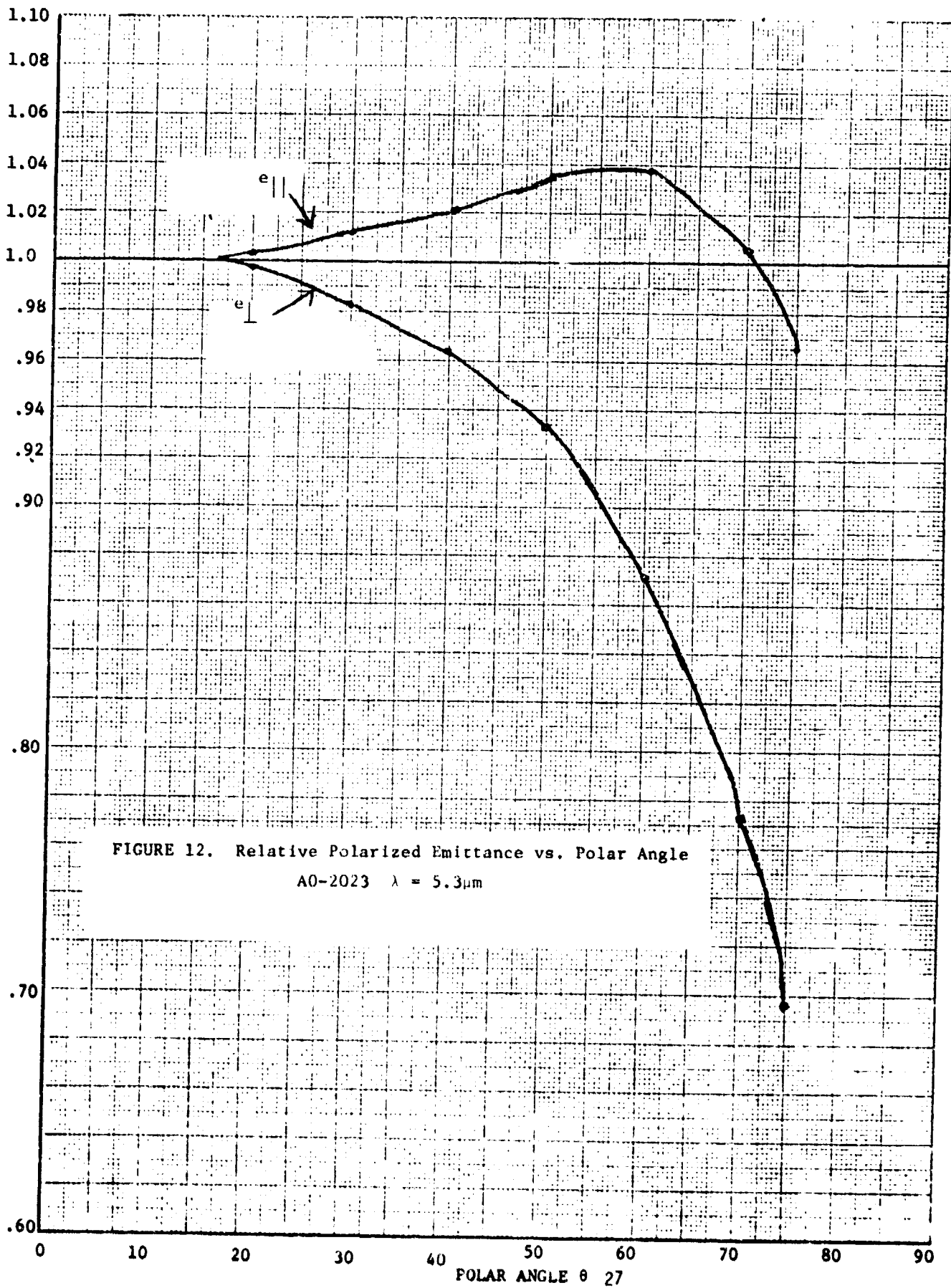


FIGURE 12. Relative Polarized Emittance vs. Polar Angle
 A0-2023 $\lambda = 5.3 \mu\text{m}$

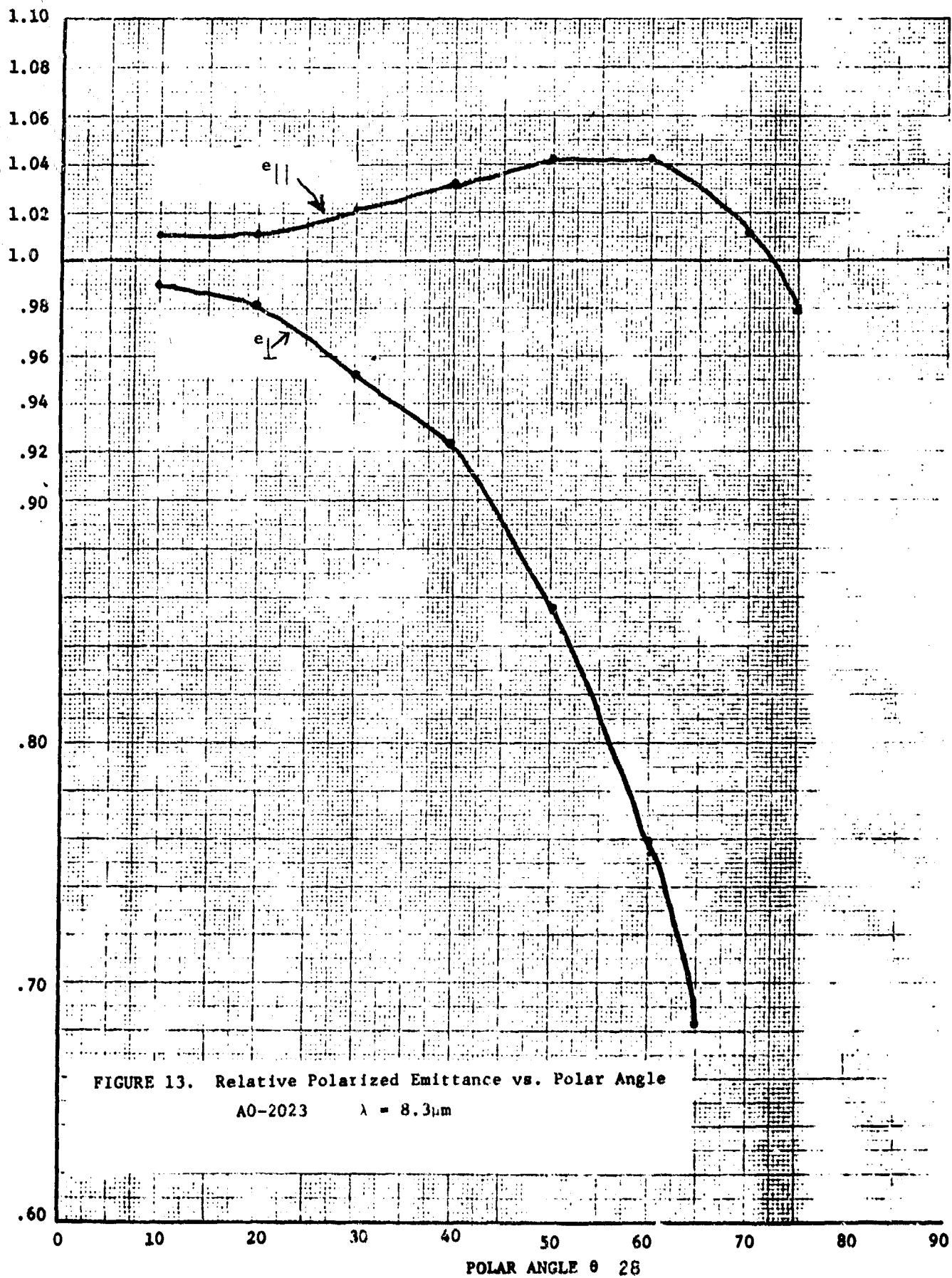


FIGURE 13. Relative Polarized Emittance vs. Polar Angle

AO-2023 $\lambda = 8.3\mu\text{m}$

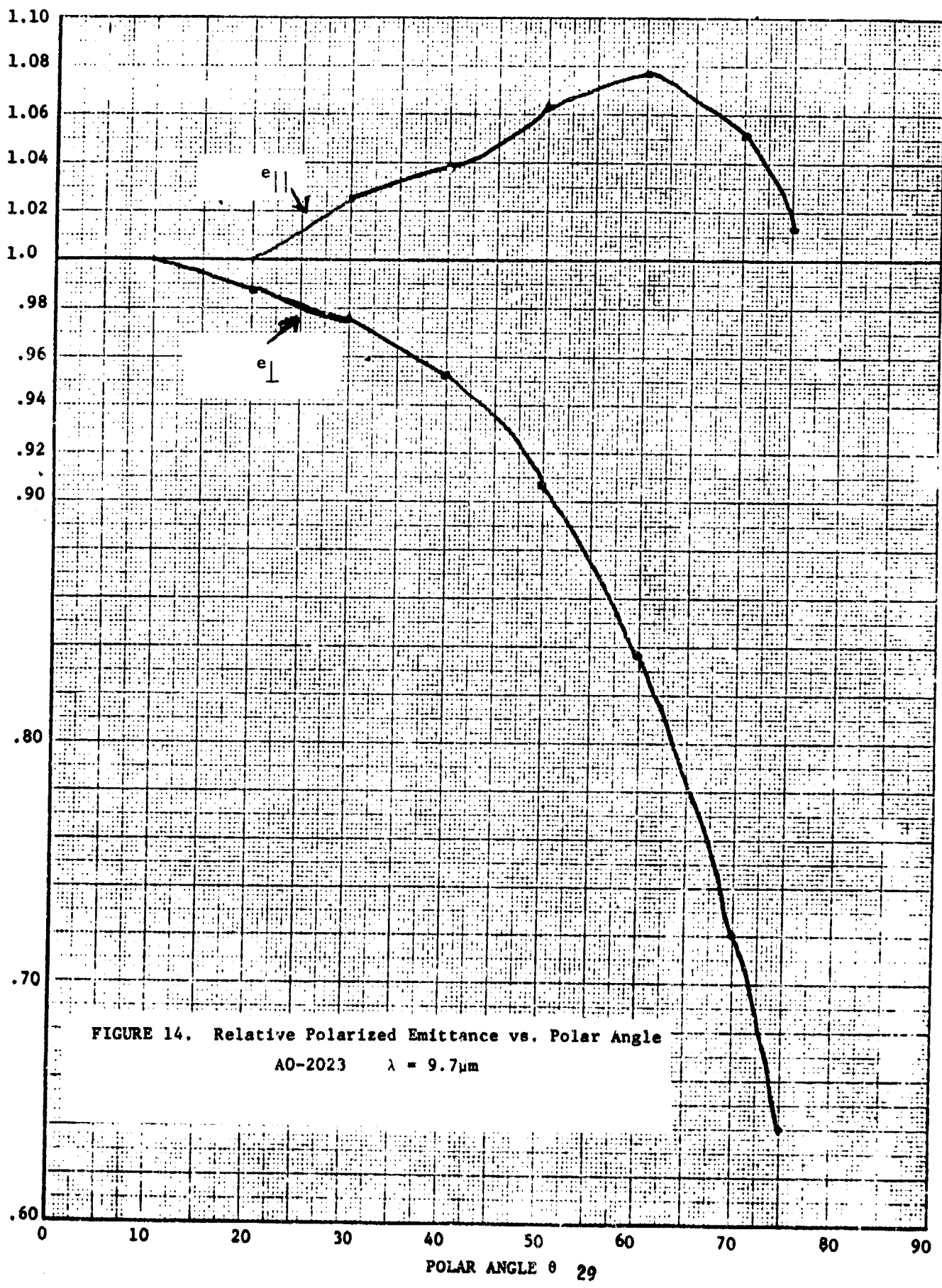


FIGURE 14. Relative Polarized Emittance vs. Polar Angle
 AO-2023 $\lambda = 9.7\mu\text{m}$

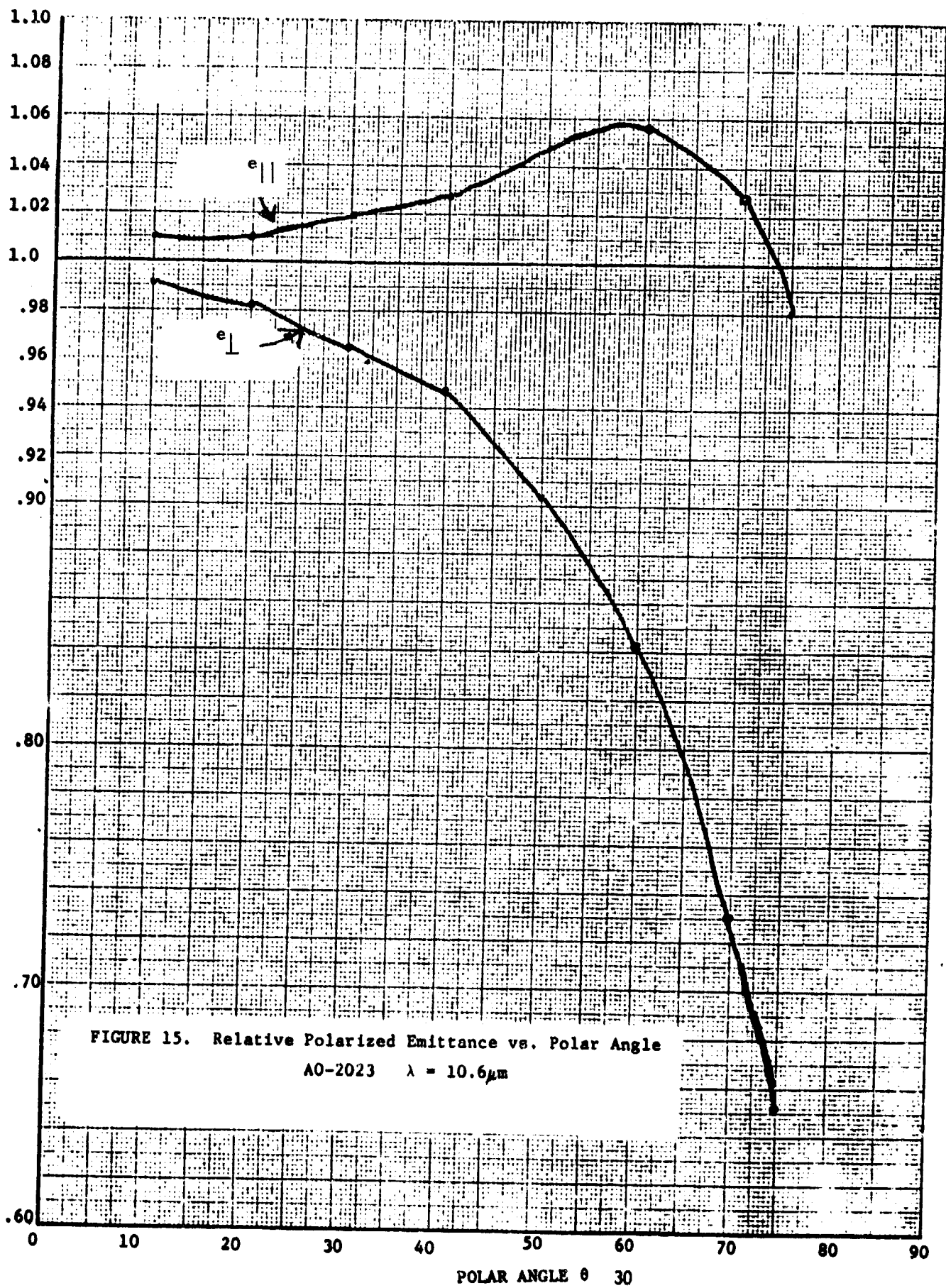
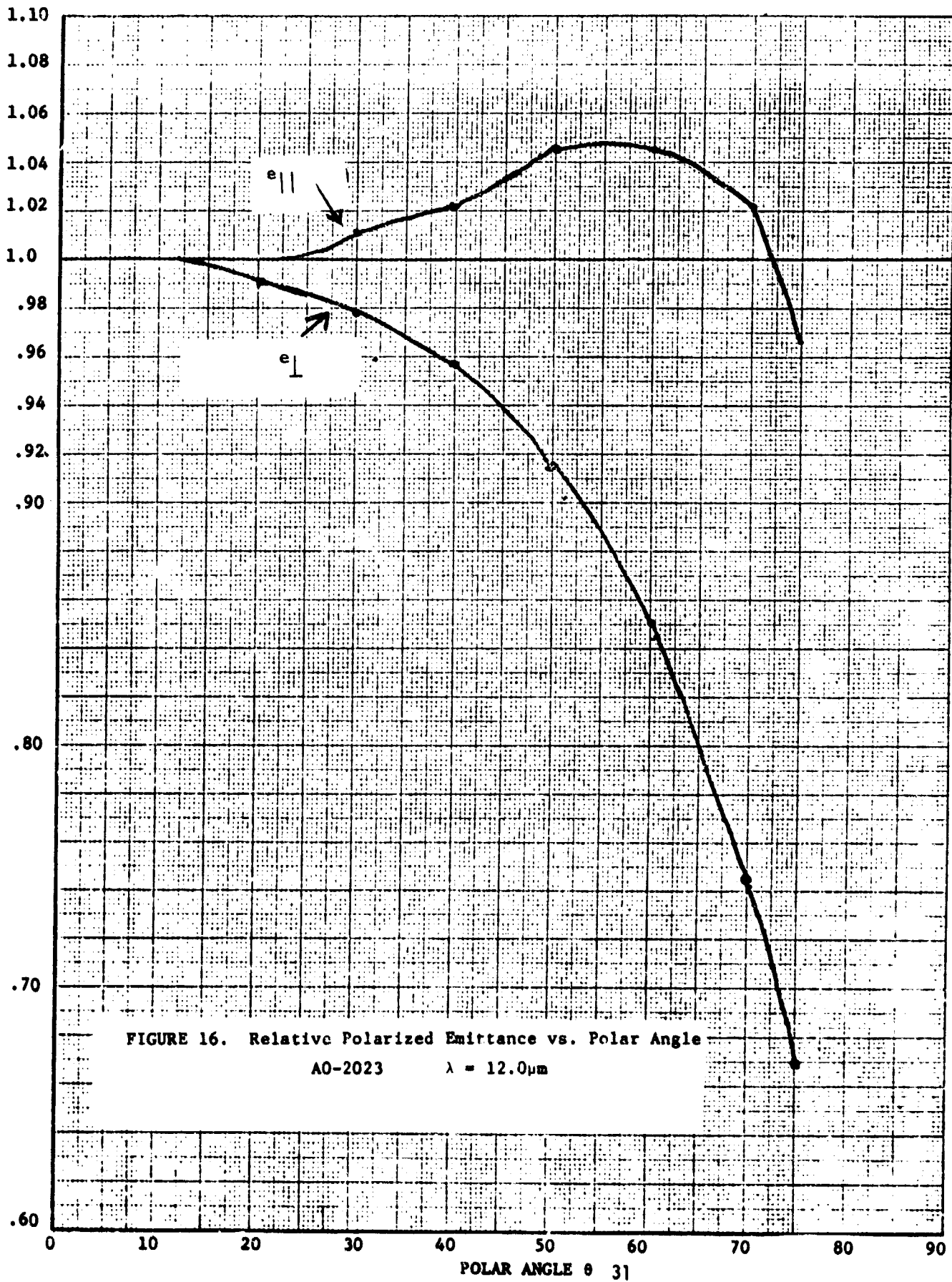


FIGURE 15. Relative Polarized Emittance vs. Polar Angle
 AO-2023 $\lambda = 10.6\mu\text{m}$



4. MODEL VALIDATION

Figure 17 shows results of the emittance model for an O. D. paint, calculated last year as part of the Target Signature Analysis Program of ERIM, for the U. S. Air Force. In this figure the degree of polarization of the emittance of an O. D. paint sample was calculated as a function of wavelength for the case of no reflective input other than clear sky radiance. The target was assumed to be at a temperature $T = 300^\circ\text{K}$ and the angle of observation was chosen to be $\theta_r = 70^\circ$. In this theoretical treatment, the paint was assumed to be a perfectly specular surface, with negligible volume and multi-surface reflection. A normal-incidence reflectivity curve was fit with the classical oscillator model discussed above to find values for the complex index of refraction $N = n - ik$ as a function of wavelength. These indices were then fed into Fresnel equations for $R_{||}$ and R_{\perp} (Eq. 3) from which $E_{||}(\theta)$ and $E_{\perp}(\theta)$ were calculated from Eq. (2). Emission polarization was then calculated from Eq. (1).

The degree of polarization of most naturally-occurring materials is low in the thermal IR, compared to the polarization of painted surfaces. The only known measurements of emission polarization from natural materials are given in Table I, which shows the degree of polarization for a few natural targets measured broadband (approximately 8 to $14\mu\text{m}$) under clear, humid sky conditions [3]. The highest degree of polarization is approximately 2% for these materials, as compared with approximately 9% for an O.D. paint sample measured at the same angle ($\theta = 75^\circ$) under the same conditions. Had the measurements been in a $2\mu\text{m}$ -wide band centered near $9.8\mu\text{m}$, Figure 17 predicts that for the O.D. paint the degree of polarization would have been appreciably higher. The increase in the degree of polarization in the reststrahlen band for target materials may be useful in the discrimination of such targets from backgrounds like water, which also can have a high degree of polarization.

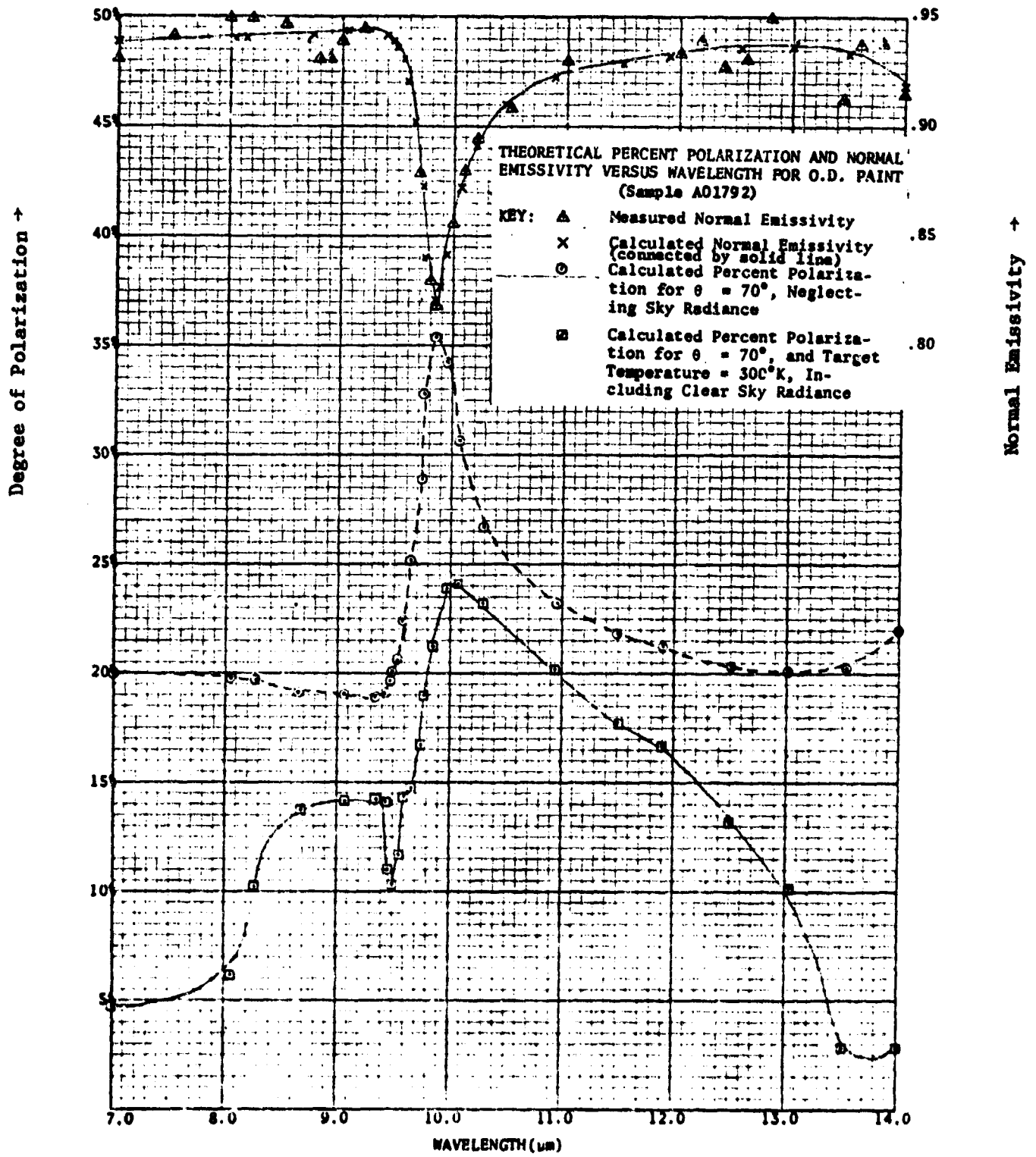


FIGURE 17

TABLE I
POLARIZATION FIELD MEASUREMENTS

(August 5, 1970, Clear
Sky Conditions, Willow
Run Airport)

Name	θ (Measured from average macroscopic surface nor- mal)	L_{\parallel} ($\frac{\text{mW}}{\text{cm}^2 \text{sr}}$)	L_{\perp} ($\frac{\text{mW}}{\text{cm}^2 \text{sr}}$)	$\frac{L_{\parallel} - L_{\perp}}{L_{\parallel} + L_{\perp}}$
Packed Beach Sand	75°	4.80	4.63	.0180
Packed Beach Sand	60°	4.88	4.82	.0062
Wet Sand	75°	5.08	4.88	.0208
Granite Rock (Irregular shape, nat- ural surface)	75°	5.37	5.16	.0199

L_{\parallel} = detected radiance from target with electric vector vibrating parallel to plane of emission

L_{\perp} = detected radiance from target with electric vector vibrating perpendicular to plane of emission

For the natural materials in Table I, the degree of polarization generally increased with increasing observation angle for $\theta > 50^\circ$, but the measured polarization was so slight for $\theta < 50^\circ$ that it fell below noise levels of the radiometer system. As for angular dependence of polarization from O. D. paint, Table II gives measured and calculated values for the degree of polarization of the emittance for θ from 10° to 70° for a wavelength of $9.83\mu\text{m}$, the center of the reststrahlen band. For $\theta > 40^\circ$ the emission polarization of paints can be quite large compared with that of natural target materials.

The good agreement between calculated results and the measured values shown in Table II were encouraging enough to justify further validation with respect to other O.D. paint samples. Under this BRL contract, three O.D. painted surfaces were studied using an ERIM spectrometer which enabled us to measure spectral radiance distributions as well as polarization dependent radiance as a function of observation angle. The samples are labeled 2017, 2022, and 2023.

Compared with the earlier sample (1792), these three O.D. paints exhibited less pronounced reststrahlen bands; hence, their degree of polarization is neither as large or as wavelength dependent. Table III shows the measured and calculated (from the above model) degree of polarization for the three O.D. paints 2017, 2022, and 2023 at angular increments of 10° for wavelengths of $10.6\mu\text{m}$, $12.0\mu\text{m}$, $9.7\mu\text{m}$, $8.3\mu\text{m}$, and $5.3\mu\text{m}$. No calculations were made for the $5.3\mu\text{m}$ wavelength primarily because the data were very noisy below $7\mu\text{m}$.

As can be observed from the "Model Result" and "Measured" columns, the model always predicts a higher degree of polarization than is measured, owing to the assumptions in the model that the paint surfaces are perfectly smooth and that the paint layer is optically thick. The middle column under each paint sample shows the product of multiplying the sample result times a constant factor of 0.75. The physical reason for choosing a constant

correction factor is that the surface roughness should affect radiation from all wavelengths and angles about the same, if the roughness is on a much different scale of magnitude than the wavelength variation (5 μ m - 12 μ m) used for the calculations of this model. The magnitude of the constant factor, however, was chosen solely on an empirical basis. As shown in Table III, the product of the model result and the 0.75 factor is within experimental error of the polarization measurements for 6 of 6 measurements on O. D. paint 2017, for 22 of 28 measurements on O.D. paint 2022, and for 15 of 27 measurements on O.D. paint 2023. The calculation of experimental error is explained in Appendix A. Overall, these calculated results for three paint samples and 4 wavelengths fell within experimental error for 43 of 61 measurements, or 70% of the time. On this basis, the model (including the 0.75 constant multiplicative factor) has been verified for degree of polarization calculations.

Figures 18, 19, and 20 are plots of relative polarized emittance versus polar angle at $\lambda = 10.6\mu$ m for O.D. paints 2017, 2022, and 2023 respectively. They show how the parallel and perpendicular components of emittance calculated by the model compared with experimental measurements. No multiplicative or other factors have been employed to alter the oscillator model results in these figures. The relative polarized emittances are

$$e_{||}(\theta) = \frac{E_{||}(\theta)}{E(0)} \quad \text{and} \quad e_{\perp}(\theta) = \frac{E_{\perp}(\theta)}{E(0)}. \quad \text{Figure 18 shows a good correlation between theoretical and observed relative polarized emittances for paint 2017, where 4 unpolarized, near-normal spectral emittance curves were averaged to produce the input for the oscillator model. Figure 19 shows what can happen when the unpolarized spectral emittance curves have measurement discrepancies. An average of the best two curves was used as oscillator model input to produce the dashed line. The two worst curves were used to produce the results shown by the rectangles, and the circles show what happens when all four curves are averaged prior to application of the$$

TABLE II

COMPARISON OF THEORETICALLY CALCULATED AND
EXPERIMENTALLY MEASURED DEGREE OF POLARIZATION
FOR EMITTANCE FOR $\lambda = 9.83\mu\text{m}$
(O.D. Paint A01792)

θ	Calculated Degree of Polarization	Measured Degree of Polarization
10°	0.58%	0.25%
20°	2.37%	1.06%
30°	5.45%	3.47%
40°	10.03%	7.50%
50°	16.35%	12.56%
60°	24.71%	20.25%
70°	35.44%	32.46%

TABLE III
COMPARISON OF THEORETICALLY CALCULATED AND EXPERIMENTALLY
MEASURED DEGREE OF POLARIZATION FOR O.D. PAINTS

		O.D. Paint A02017			O.D. Paint A02022			O.D. Paint A02023		
θ		Calculated (%)		Measured (%)	Calculated (%)		Measured (%)	Calculated (%)		Measured (%)
		Model Result	Multiplied by 0.75		Model Result	Multiplied by 0.75		Model Result	Multiplied by 0.75	
$\lambda = 10.6\mu\text{m}$	10°	0.3	0.2	0.3±1.9	0.3	0.2	0.3±1.5	0.6	0.5	0.9±1.8
	20°	1.4	1.0	1.9±1.9	1.3	1.0	1.0±1.5	2.3	1.7	1.4±1.8
	30°	3.3	2.5	2.8±1.9	2.1	2.3	2.2±1.5	5.1	3.8	2.7±1.8
	40°	6.1	4.6	4.5±1.9	5.7	4.3	4.3±1.5	9.0	6.8	4.1±1.8
	50°	10.2	7.7	7.7±1.9	9.5	7.1	7.0±1.5	19.7	10.3	7.3±1.8
	60°	15.9	11.9	12.3±2.0	14.6	11.0	11.4±1.6	19.2	14.4	11.3±1.9
	70°	23.7	17.8	-	21.4	16.1	16.7±1.7	25.5	19.1	17.0±2.1
$\lambda = 12.0\mu\text{m}$	10°			0.3	0.2	<0.3±1.9	0.4	0.3	<0.5±2.0	
	20°			1.1	0.8	0.7±1.9	1.8	1.4	<0.5±2.0	
	30°			2.6	2.0	2.6±1.9	4.1	3.1	1.6±2.0	
	40°			5.0	3.8	4.5±1.9	7.5	5.6	3.3±2.0	
	50°			8.4	6.3	7.5±1.9	12.0	9.0	6.6±2.0	
	60°			13.3	10.0	12.0±2.0	17.6	13.2	10.2±2.1	
	70°			20.0	15.0	18.0±2.2	24.7	18.5	15.7±2.3	
$\lambda = 9.7\mu\text{m}$	10°			0.4	0.3	<0.3±2.0	0.7	0.5	<0.5±2.0	
	20°			1.7	1.3	1.3±2.0	2.7	2.0	<0.5±2.0	
	30°			3.8	2.9	2.9±2.0	5.9	4.4	2.4±2.0	
	40°			6.9	5.2	5.4±2.0	10.0	7.5	4.6±2.0	
	50°			11.0	8.3	9.7±2.0	14.7	11.0	8.0±2.0	
	60°			16.2	12.2	14.6±2.1	19.8	14.9	12.5±2.1	
	70°			22.6	17.2	21.7±2.4	25.3	19.0	18.6±2.4	
$\lambda = 8.3\mu\text{m}$	10°			0.4	0.3	<0.3±1.8	0.8	0.6	1.0±1.9	
	20°			1.8	1.4	0.7±1.8	3.3	2.5	1.6±1.9	
	30°			4.2	3.2	2.0±1.8	7.1	5.3	3.5±1.9	
	40°			7.4	5.6	3.5±1.8	11.5	8.6	5.6±1.9	
	50°			11.3	8.5	6.3±1.8	15.9	11.9	9.8±1.9	
	60°			15.4	11.6	9.5±1.9	20.0	15.0	15.6±2.0	
	70°			19.6	14.7	15.0±2.1	23.8	17.9	-	
$\lambda = 5.3\mu\text{m}$	10°					0.2			-	
	20°					0.8			0.3	
	30°					1.8			1.5	
	40°					3.2			3.9	
	50°					5.5			5.1	
	60°					9.0			8.7	
	70°					13.9			11.1	

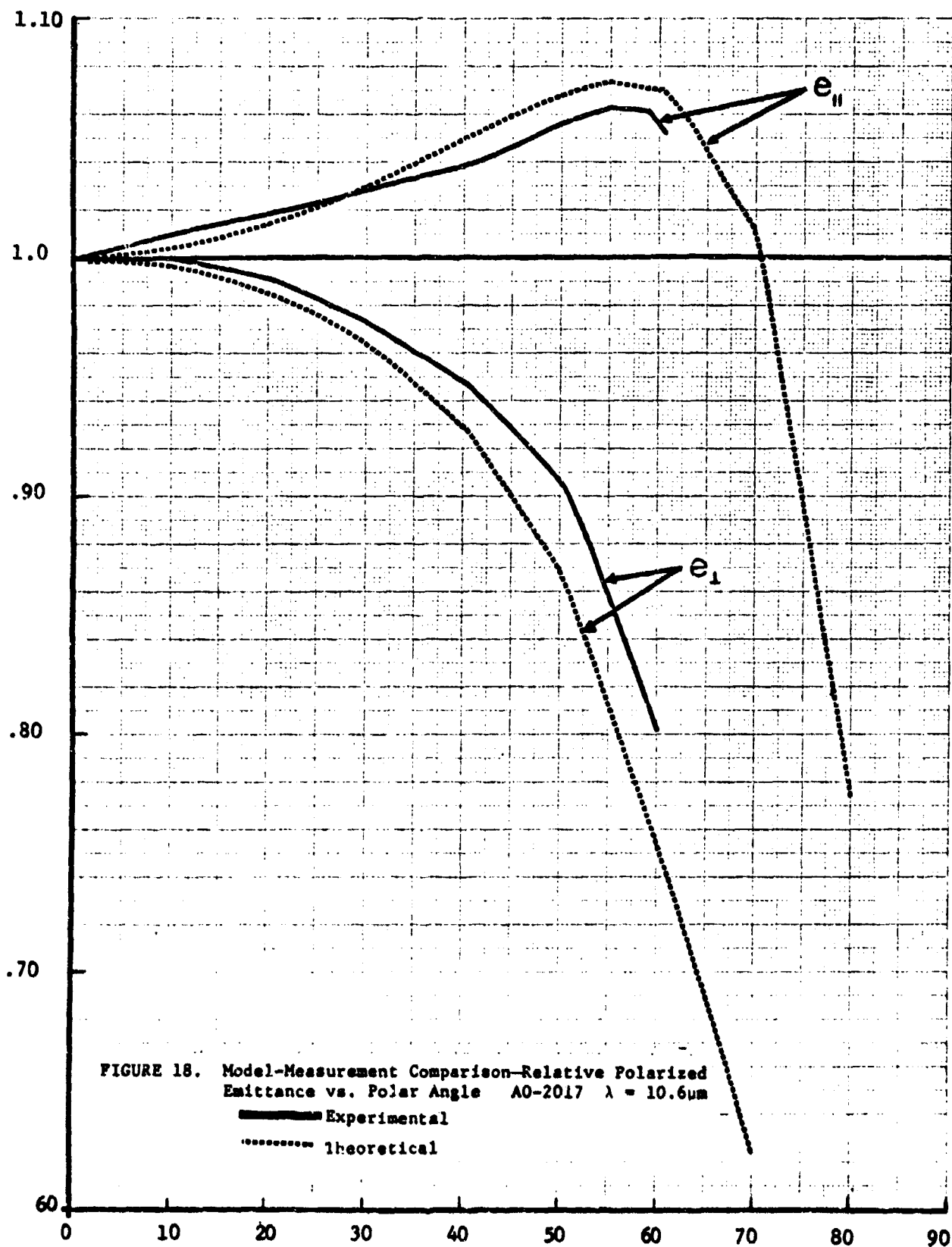
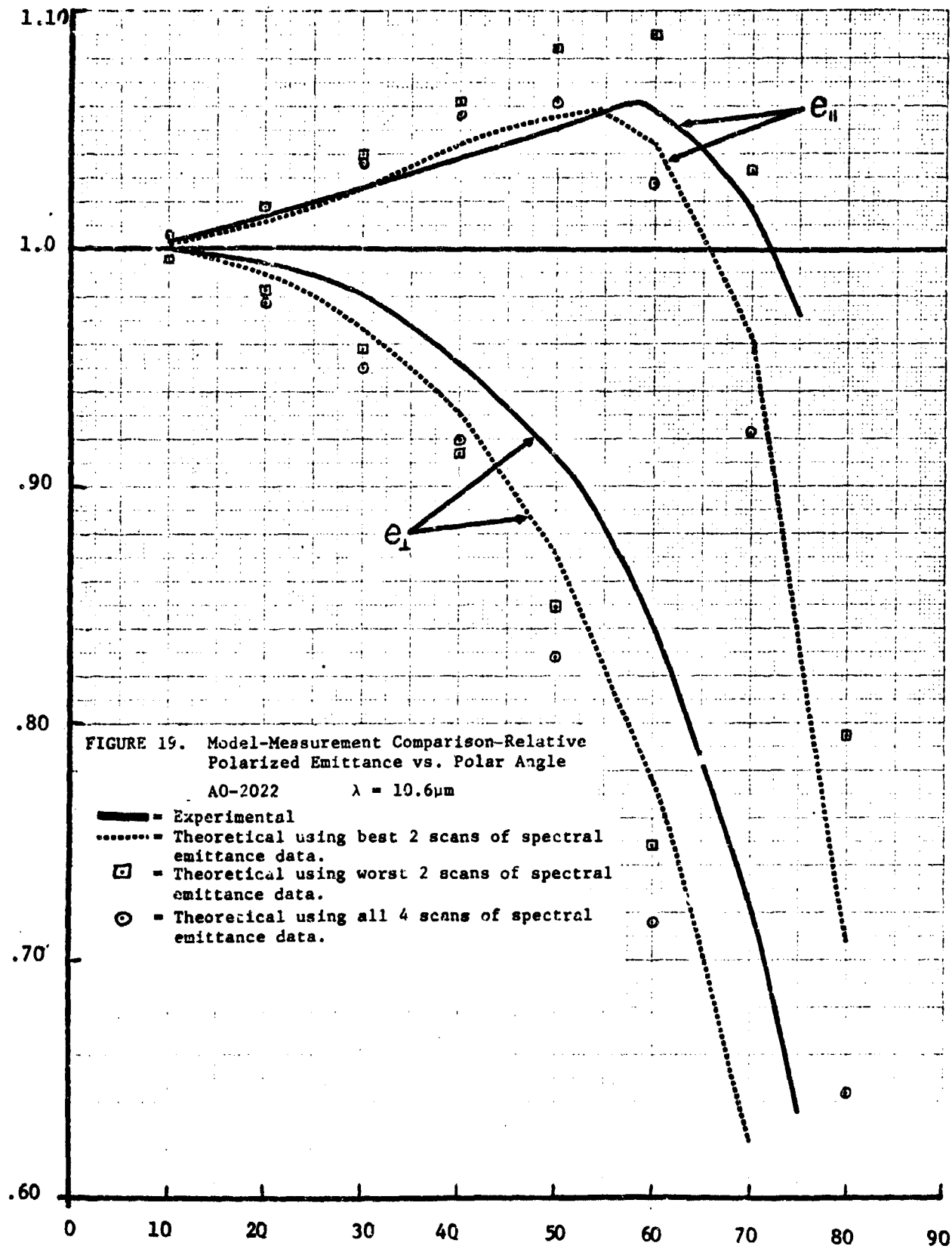
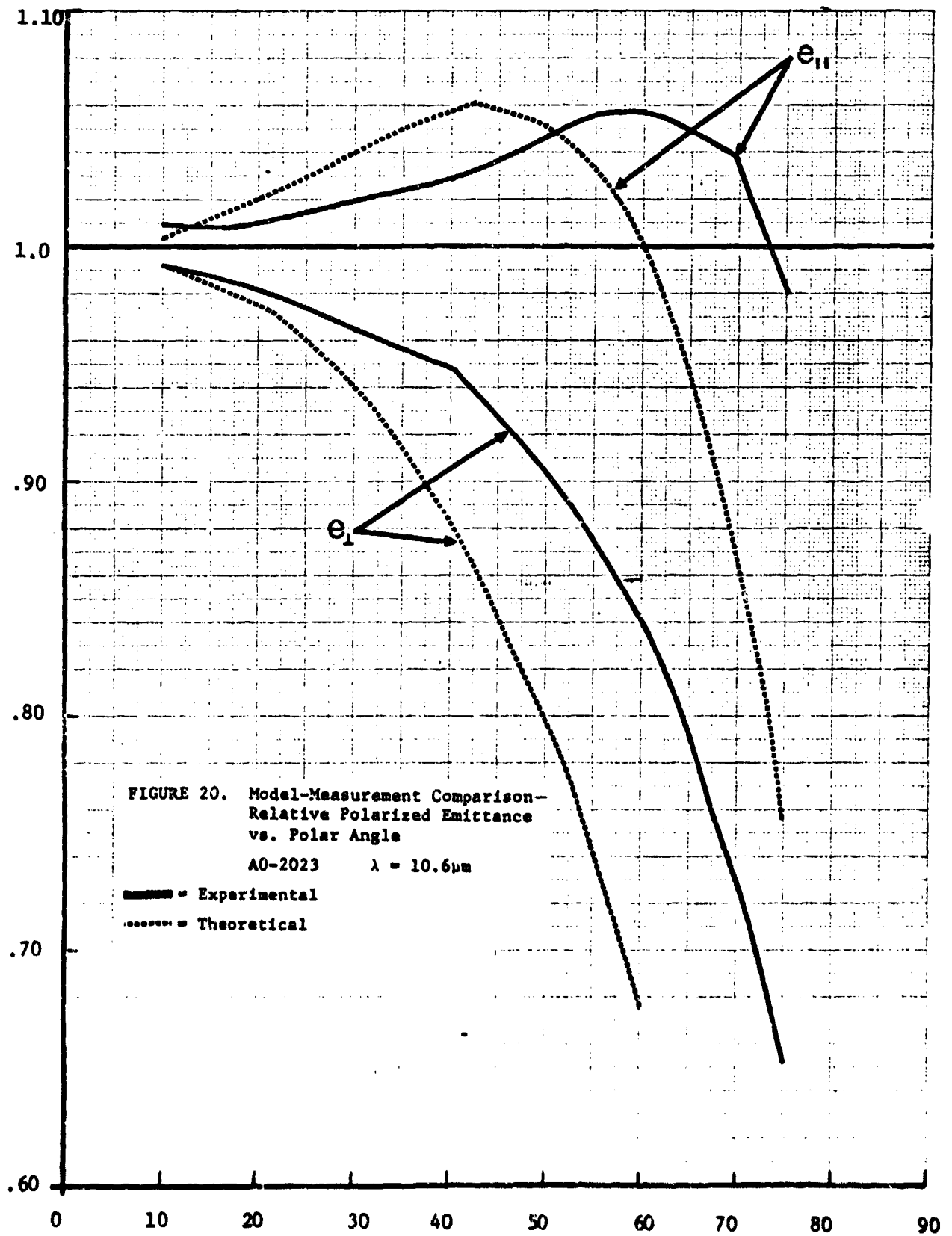


FIGURE 18. Model-Measurement Comparison—Relative Polarized Emittance vs. Polar Angle AO-2017 $\lambda = 10.6\mu\text{m}$

— Experimental

..... theoretical





oscillator model. This points out the need for better spectral emittance measurements as inputs to the model. Figure 20 shows the poorer results with paint 2023. The oscillator model was applied twice to the average of 4 spectral emittance curves, with almost the same results. The poorer agreement in Figure 20 is obvious also in the smaller than expected calculated degree of polarization results of Table III for paint 2023.

5. CONCLUSIONS

The oscillator model for calculating polarized components of spectral emittance and degree of polarization in the thermal infrared region for smooth-surfaced targets has produced theoretical values that are within experimental measurement accuracy 70% of the time. The accuracy of the model could be improved with better measurements of unpolarized, near-normal spectral emittance values. Such measurements could be improved by utilizing a parabolic reflectometer in the reflection mode instead of FISR, in the emission mode because of the greater absolute accuracy afforded by the former. FISR measurements would still probably be preferred for the relative polarized emittance versus polar angle measurements, because of the induced polarization inherent to the parabolic reflectometer. The model itself could probably be improved by accounting for thin-film transmission of paint on metal, but this might not be required after better spectral emittance measurements are available.

Although the O.D. paints used in this investigation are similar in spectral emittance features, the oscillator model should work at least as well for other smooth-surfaced materials which exhibit marked dispersion (high λ -dependence of the spectral emittance) in the thermal IR region, such as teflon, mylar, and possibly phenolics.

The most important feature of this model is that the degree of polarization can be calculated for smooth-surfaced materials in the thermal IR region for any λ (from about 7 to 15 μ m) and any polar angle, with only a measurement of spectral emittance from 7 - 15 μ m at near-normal incidence required. This will save considerable time and money on experimental measurements.

APPENDIX A

DETERMINATION OF EXPERIMENTAL ERROR IN MEASUREMENT OF DEGREE OF POLARIZATION

The equation for degree of polarization can be written as:

$$P_E(\theta) = \frac{E_{||}(\theta) - E_{\perp}(\theta)}{E_{||}(\theta) + E_{\perp}(\theta)} = \frac{e_{||}(\theta) - e_{\perp}(\theta)}{e_{||}(\theta) + e_{\perp}(\theta)} \quad (A-1)$$

where $e_{||}(\theta) = \frac{E(\theta)_{||}}{E(0)}$ = relative polarized emittance, parallel component

$e_{\perp}(\theta) = \frac{E(\theta)_{\perp}}{E(0)}$ = relative polarized emittance, perpendicular component

All of the above and following parameters are wavelength and angle dependent, but the λ and θ notation will be suppressed here.

The error in P_E due to errors in measured values of $e_{||}$ and e_{\perp} , respectively, can be represented by:

$$\Delta P_{E_{||}} = \left[\frac{1}{e_{||} + e_{\perp}} - \frac{e_{||} - e_{\perp}}{(e_{||} + e_{\perp})^2} \right] \Delta e_{||} = \frac{2e_{\perp}}{(e_{||} + e_{\perp})^2} \Delta e_{||} \quad (A-2)$$

$$\Delta P_{E_{\perp}} = \left[-\frac{1}{e_{||} + e_{\perp}} - \frac{e_{||} - e_{\perp}}{(e_{||} + e_{\perp})^2} \right] \Delta e_{\perp} = \frac{-2e_{||}}{(e_{||} + e_{\perp})^2} \Delta e_{\perp} \quad (A-3)$$

The total error in P_E can be described as:

$$\Delta P_E = \sqrt{(\Delta P_{E_{||}})^2 + (\Delta P_{E_{\perp}})^2} = \left[\frac{2}{(e_{||} + e_{\perp})^2} \right] \sqrt{(e_{\perp} \Delta e_{||})^2 + (e_{||} \Delta e_{\perp})^2} \quad (A-4)$$

Let σ_p be the precision error in the measurement of unpolarized spectral emittance. It will be assumed that $\Delta e_{||}$ and Δe_{\perp} are equal and that the addition of a polarizer into the optical system increases the precision

error by a factor of $\sqrt{2}$, such that

$$\Delta e_{||} = \Delta e_{\perp} = \sqrt{2} \sigma_p \quad (\text{A-5})$$

When equation (A-5) is substituted into equation (A-6), the resultant error in P_E from error measurements in $e_{||}$ and e_{\perp} is:

$$\Delta P_E = \frac{2\sigma_p}{(e_{||} + e_{\perp})^2} \sqrt{2(e_{||}^2 + e_{\perp}^2)} = 2.828 \sigma_p \frac{\sqrt{e_{||}^2 + e_{\perp}^2}}{(e_{||} + e_{\perp})^2} \quad (\text{A-6})$$

The ΔP_E is multiplied by 100 in Table III to get % ΔP_E . It can be observed from equation (A-6) that ΔP_E is not a strong function of the values of $e_{||}$ and e_{\perp} , and that $\Delta P_E \approx 2.828\sigma_p$ for small θ , where $e_{||}$ and e_{\perp} are near 1.0 in value.

APPENDIX B
DOCUMENTATION FOR CLASSICAL
OSCILLATOR FITTING PROGRAM

The oscillator fitting program is designed to compute oscillator parameters from which effective indices of refraction can be calculated, according to Eq. (1) of the text. Initial estimates of the number of oscillators responsible for spectral features of the specimen and the strengths (S), frequency positions ($NU = \frac{\lambda}{10,000}$, for λ in μm), and widths (GAMMA) of each oscillator must be made. The dielectric constant at infinite frequency (E) must also be made known. [Note: Here $E = E_{\infty}$.]

To begin with one assumes at least one oscillator is located at each reflectance maximum in the infrared reflectance spectrum. This determines the initial number of oscillators and their positions (NU). The initial values of E, S, and GAMMA can be taken to be equal to the values determined for the O.D. paint 2017 in Table B-1. Table B-1 gives the result of the oscillator fitting program for the three O.D. paints listed in Table 1 of the text.

The program will refine the position, strength, and shape of the given oscillators, but it will not add or delete oscillators. However, if an oscillator is grossly superfluous, the strength will be decreased, and/or the width will be increased, to such an extent as to make its contribution negligible.

The program returns an error parameter before supplying the new oscillator parameters. If the error parameter is 0, convergence (under the input EPS and EST^{*}) has taken place, otherwise it has not. Whether or not convergence has taken place, it is often advisable to look at the oscillator parameters and the emittance values calculated from them to decide if additional oscillators should be added and/or subtracted, or whether the limiting conditions (ESP, EST) should be changed. If the theoretical and experimental reflectance curves do not quantitatively match, i.e. do not peak and trough near the same wavelengths, addition or subtraction of an oscillator is called for. In general, two things are

^{*}See last page of this Appendix for definitions.

necessary to judge a good fit: a sum of the differences squared (between theoretical and experimental spectral reflectance) less than about 10^{-2} and a qualitative match between peaks and valleys of experimental and theoretical spectral reflectance curves. For low-contrast materials (small reststrahlen bands), a good quantitative fit is usually not a sufficient criterion for successful fitting, as seen by the results for sample 2023 in Table B-1 and Table 1 of the text. (See discussion in text of Appendix C.)

TABLE B-1

EFFECTIVE OSCILLATOR PARAMETERS FOR POINTS RESULTING
FROM CLASSICAL OSCILLATOR FITTING PROGRAM

O. D. Paint Sample	Oscillator Parameters			
	E	S	NU	GAMMA
A02017	1.040	0.5421	993.7	0.3234
		0.1053	1373.9	0.4264
A02022	1.051	0.0866	787.8	0.1190
		0.5716	988.4	0.4168
A02023	.728	1.076	828.0	.7384
		.2456	1022.6	4.683

DATA DECK FOR THE OSCILLATOR PROGRAM

<u>CARD #</u>	<u>FORMAT</u>	<u>VARIABLES(s)</u>	<u>DESCRIPTION</u>
1	20A4	A	Any title up to 80 characters in length (including blanks).
2	I5, E15.5, and F10.0	LIMIT, EPS, EST	LIMIT = number of iterations desired (30 is a good choice); EPS = test value for the expected absolute error (see the write-up on FMFP; despite what it says 0.05 has worked reasonably well); EST = estimated value of F(x) (also see Appendix F).
3	I5	N	Three times the number of cards of type 4, plus 1 (i.e., total number of parameters needed to describe all the oscillators with card types 4 and 5).
4	3F10.0	S, NU, GAMMA	S = strength of the oscillator; NU = location of the oscillator (in wave numbers); GAMMA = width of oscillator.
5	F10.0	E	Dielectric constant at infinite frequency.
6	I5	M	Number of points used to describe the curve (i.e., no. of cards of type 7).
7	2F10.0	WIN(I), RIN(I)	WIN(I) = wave number for the data point; RIN(I) = percent emittance at WIN(I). Use as many of these as necessary to thoroughly delineate the curve (at least 45-50).

APPENDIX C

DOCUMENTATION FOR PROGRAM 'EMISPOL'.

EMISPOL is a straightforward program, in which the oscillator parameters from the previous program are input parameters. Output is degree of polarization (PERPOL) and $e_{||}(\theta)$ and $e_{\perp}(\theta)$, relative emittance components.

Where reststrahlen bands are small, it is important to note that the index of refraction as determined by the oscillator program is not reliable. If band structure is not pronounced it is difficult to determine suitable oscillator parameters. On the other hand, the emissivity is then not very spectrally dependent, which means that it is reasonable to regard the refractive index as constant over the same wavelength region.

Under these circumstances it is valid to by-pass the oscillator program and feed a constant value for refractive index into EMISPOL. Doing so requires a slight modification of EMISPOL. Immediately after statement 600 (see EMISPOL listing in Appendix E), the program calls in a subroutine which calculates n and k given the final oscillator parameters. This subroutine (and hence the oscillator program) can be by-passed by substituting a statement which supplies values for n and k . Values can be determined from the Brewster angle as described in Volume I of this report.

DATA DECK FOR EMISPOL

<u>CARD #</u>	<u>FORMAT</u>	<u>NAME</u>	<u>DESCRIPTION AND/OR COMMENTS</u>
1	10A4	ITITLE	Any title information, up to 80 characters.
2	I3	K	No. of Lamdas (wavelengths) to be provided (a maximum of 185; see card 10).
3	F5.3	EPS	E from Program OSSC.
4	I2	NPTS	No. of Oscillators (a maximum of 8).
5	7F8.2	FR(I)	NU values from Program OSSC.
6	7F8.4	S(I)	S values from Program OSSC.
7	7F8.4	G(I)	GAM values from Program OSSC.
8	I3	M	No. of AI's (a maximum of 10) (see card 11).
9	I3	T	Temperature of the object which is emitting (in degrees K).
10	10F8.3	LAMDA(J)	Lamda's at which emittance polarization is calculated for each AI(N).
11	F10.6	AI(N)	Angles of incidence (1 per card).

APPENDIX D
PROGRAM LISTING - OSCILLATOR

```

DIMENSION RFD(13,600),D1(602),D2(602)
DIMENSION WIN(300),RIN(300)
DIMENSION LABEL(6)
DIMENSION LBL(9),LBI(9),LBM(2)
REAL XS(25),H(27)
REAL X(25),G(25),D(1000),A(20),DATA(250)
DATA LBL/36H          ALPHA          /
DATA LABEL/4H R ,4H E1 ,4H E2 ,4H EF ,4H N ,4H K /
C .....
548 READ(5,548)A,LIMIT,EPS,EST
C .....
555 FORMAT(20A4,/,I5,E15.5,F10.0)
C .....
555 READ(5,555)N
555 FORMAT(I5)
C .....
555 READ(5,555)(X(I),I=1,N)
555 FORMAT(3F10.0)
-----
40 WRITE(6,40)A,LIMIT,EPS,EST
40 FORMAT(1H1,20A4,/' LIMIT OF ITERATIONS IS',I5,' EPS IS ',E15.5,/'
.' ESTIMATED F(X)= ', F12.5,/)
C .....
470 WRITE(6,470)
470 FORMAT(5X,'INITIAL GUESSES FOR OSCILLATOR PARAMETERS ARE '//)
NM=N-1
C .....
471 WRITE(6,471) (X(I),I=1,NM)
471 FORMAT(14X,'S',16X,'NU',14X,'GAMMA',/(5X,E12.5,8X,E12.5,
. 8X,E12.5))
C .....
472 WRITE(6,472)X(N)
472 FORMAT(3X, 'E(INF)= ',F12.4)
C .....
555 READ(5,555) M
C .....
1766 WRITE(6,1766)N
1766 FORMAT(' CARD COUNT IS ',I5)
C .....
2000 WRITE(6,2000)
2000 FORMAT(' REFLECTIVITY BASED ON INITIAL GUESSES'//)
C .....
555 WRITE(6,487)
555 .....
555 READ(5,555)(WIN(I),RIN(I),I=1,M)
555 FORMAT(2F10.0)
29 DO 29 I=1,N
29 X(I)=SQRT(X(I))
ZTL=0
DO 10 J=1,M
RIN(J)=RIN(J)/100.
YY=FUNX(I,X,WIN(J))
Z=YY-RIN(J)
ZLT=ZLT+Z*Z
C .....
10 WRITE(6,10) WIN(J),RIN(J),YY,Z
10 CONTINUE
C .....
1112 WRITE(6,1112)ZLT
1112 FORMAT(5X,' SUM OF THE DIFFERENCES SQUARED IS ',E12.4)
CALL FUNCT(M,WIN,RIN)

```

```

EXTERNAL FUNCT
IF(LIMIT .EQ. 0)GO TO 250
CALL FMFP(FUNCT,N,X,F,G,EST,EPS,LIMIT,IER,B)
250 CONTINUE
DO 19 I=1,N
19 XS(I)=X(I)**2
C -----
WRITE(6,9745)
9745 FORMAT(1H1)
C -----
WRITE(6,473)F,IER
.473 FORMAT(3X,///'FITTING HAS BEEN COMPLETED WITH F(X)= ',E15.8,/'
.' AND ERROR PARAMETER = ',I5/' FITTED VALUES FOR OSCILLATOR',
.' PARAMETERS ARE '/')
C -----
WRITE(6,471)(XS(I),I=1,NM)
WRITE(6,472)XS(N)
WRITE(6,487)
487 FORMAT(1H1,3X'ENERGY          R(EXP)          R(FITTED)  DIFFERENCE'/)
ZLT=0
DO 13 J=1,M
YY=FUNX(N,X,WIN(J))
Z=YY-RIN(J)
ZLT=ZLT+Z**2
C -----
WRITE(6,16)WIN(J),RIN(J),YY,Z
16 FORMAT(1X,4F12.5)
13 CONTINUE
C -----
WRITE(6,1112)ZLT
END

```

```

SUBROUTINE FUNCT(M,WIN,RIN)
DIMENSION WIN(300),RIN(300)
RETURN
ENTRY FUNCT(N,X,VAL,GRAD)
REAL X(25),GRAD(25)
REAL W(10),S(10),G(10)
REAL P(300),Q(300),V(300)
COMPLEX Z,O(300,10),E(300),H(300)
NN=N/3
DO 1 I=1,NN
L=3*(I-1)
S(I)=X(L+1)
W(I)=X(L+2)
1 G(I)=X(L+3)
EINF=X(N)
DO 2 J=1,NN
W2=1./W(J)**2
G2=C(J)**2
DO 2 I=1,M
WW=WIN(I)*W2
2 D(I,J)=S(J)/CMPLX(1.-WW**2,-WW*G2)
DO 3 I=1,M
E(I)=EINF**2
DO 4 J=1,NN

```

```

4 E(I)=E(I)+S(J)*D(I,J)
  E(I)=CEXP(.5*CLOG(E(I)))
  IF(REAL(E(I)).LT.C.)E(I)=-E(I)
  P(I)=CABS(E(I))**2-2.*REAL(E(I))+1.
  Q(I)=P(I)+4.*REAL(E(I))
3 V(I)=P(I)/Q(I)-RIN(I)
  VAL=0
  DO 33 I=1,M
33 VAL=VAL+V(I)**2
-----
C
  WRITE(6,76) VAL
76 FORMAT(1X,E14.5)
  DO 7 I=1,M
  Z=CONJG(E(I))
7 H(I)=8.*V(I)+.5*(Q(I)*(Z-1.)-P(I)*(Z+1.))/E(I)/Q(I)**2
  DO 6 J=1,NN
  L=3*(J-1)
  GRAC(L+1)=0
  GRAC(L+2)=0
  GRAC(L+3)=0
  W2=G(J)/W(J)**2
  W3=-C(J)**2/W(J)**3
  W5=-2./W(J)**5
  DO 6 I=1,M
  GRAC(L+1)=GRAC(L+1)+REAL(H(I)*D(I,J))
  Z=H(I)*D(I,J)**2*WIN(I)
  GRAC(L+2)=GRAC(L+2)+REAL(Z*CMPLX(WIN(I)*W5,W3) )
  GRAC(L+3)=GRAC(L+3)-AIMAG(Z)*W2
6 CONTINUE
  GRAC(N)=0
  DO 8 I=1,M
8 GRAC(N)=GRAC(N)+REAL(H(I))*EINF
  RETURN
  END

FUNCTION FUNX(N,X,WIN)
REAL X(25)
REAL W(10),C(10),S(10)
NN=N/3
DO 1 I=1,NN
L=3*(I-1)
S(I)=X(L+1)
W(I)=X(L+2)
G(I)=X(L+3)
1 CONTINUE
COMPLEX E
E=X(N)**2
DO 2 J=1,NN
E=E+S(J)**2/CMPLX(1.-(WIN/W(J))**2)**2,-WIN*G(J)**2/W(J)**2)
2 CONTINUE
E=CEXP(.5*CLOG(E))
IF(REAL(E).LT.0.)E=-E
FUNX=CABS((E-1.)/(E+1.))**2
RETURN
END

```

APPENDIX E

PROGRAM LISTING - EMISPOL

```

DIMENSION LAMDA(185),AN(185),AK(185),AI(10),ER(185),EL(185)
DIMENSION DE(185),NR(185),NL(185),DN(185),ITITLE(10),NSKY(9,185)
DIMENSION FR(8),S(9),G(8),EE(185)
DIMENSION PERPOL(185)
COMMON FR,S,G
COMMON NPTS,EPS
REAL LAMDA,NSKY,NTAR,NR,NL
INTEGER T
INTEGER SKY
C INPUT
100 READ (5,5) ITITLE
5 FORMAT(10A4)
WRITE (6,6) ITITLE
6 FORMAT (1H1,10A4)
READ (5,10) K
10 FORMAT (I3)
READ (5,12) EPS
12 FORMAT (F5.3)
READ (5,21) NPTS
21 FORMAT (I2)
READ (5,20) (FR(I),I=1,NPTS)
20 FORMAT (8F8.2)
READ (5,25) (S(I),I=1,NPTS)
25 FORMAT (8F8.4)
READ (5,25) (G(I),I=1,NPTS)
READ (5,40) M
40 FORMAT (I3)
56 READ (5,60) T
60 FORMAT (I3)
609 READ (5,610) (LAMDA(I),I=1,K)
610 FORMAT (10F8.0)
N=0
645 N=N+1
READ (5,650) AI(N)
650 FORMAT (F10.6)
AI(N)=90.0-AI(N)
DO 660 I=1,K
NSKY(N,I)=0.0
IF (N.GE.M) GO TO 600
GO TO 645
660 CONTINUE
C CALCULATIONS
600 DO 700 JJ=1,K
CALL ANAK(LAMDA(JJ),AN(JJ),AK(JJ))
700 CONTINUE
DO 200 II=1,M
AI(II)=AI(II)*3.1416/180.
DO 150 JJ=1,K
Q=SQRT(.5*(AN(JJ)**2)*(AK(JJ)**2)+((AN(JJ)**2)-(AK(JJ)**2)-SIN(AI(
1 II)**2)**2)
A=0.5*(+AN(JJ)**2-AK(JJ)**2-(SIN(AI(II)))**2+Q)
B=0.5*(-AN(JJ)**2+AK(JJ)**2+(SIN(AI(II)))**2+Q)
RR=((SQRT(A)-COS(AI(II)))**2+B)**
1 ((SQRT(A)+COS(AI(II)))**2+B)
RL=(RR*((SQRT(A)-SIN(AI(II))*TAN(AI(II)))**2+B))/
1 ((SQRT(A)+SIN(AI(II))*TAN(AI(II)))**2+B)
NTAR=1.19E4/((LAMDA(JJ)**5)*((EXP(1.4388E4/(LAMDA(JJ)*T))-1.0))
ER(JJ)=1.0-RR
EL(JJ)=1.0-RL
EE(JJ)=.5*(ER(JJ)+EL(JJ))

```

```

DE(JJ)=EL(JJ)-ER(JJ)
NR(JJ)=(RR*NSKY(II,JJ)/2.0)+(ER(JJ)*NTAR/2.0)
NL(JJ)=(RL*NSKY(II,JJ)/2.0)+(EL(JJ)*NTAR/2.0)
DN(JJ)=NL(JJ)-NR(JJ)
PERPOL(JJ)=(EL(JJ)-ER(JJ))/(EL(JJ)+ER(JJ))
150 CONTINUE
AI(II)=AI(II)*180./3.1416
WRITE (6,70) AI(II),T,(LAMBDA(L),AN(L),AK(L),NSKY(II,L),ER(L),EL(L)
1,DE(L),NR(L),NL(L),DN(L),EE(L),PERPOL(L),L=1,K)
70 FORMAT (// 'AI= ',F8.3/, 'TEMP= ',I5/,1X,'LAMBDA',3X,'AN',6X,'AK',6X
1,'NSKY',7X,'ER',9X,'EL',9X,'DE',9X,'NR',9X,'NL',9X,'DN',9X,'EE',7X
2,'PERPOL',/(F6.2,2X,F6.4,2X,F6.4,2X,E10.4,1X,E10.4,1X,E10.4,1X
3,E10.4,1X,E9.3,1X,E9.3,1X,E9.3,1X,E10.4,1X,E10.4))
200 CONTINUE
GO TO 100
END

```

```

SUBROUTINE ANAK(LAMBDA,AV,AK)
DIMENSION FR(8),S(8),G(8)
COMMON FR,S,G
COMMON NPTS,EPS
REAL LAMBDA
F=10000./LAMBDA
AE=C.
BB=0.
DO 110 KK=1,NPTS
QC=(S(KK)*((FR(KK))**2))/(((FR(KK))**2-F**2)**2+(G(KK)*FR(KK)*F)**
12)
AE=CQ*((FR(KK))**2-F**2)+AE
BB=(.5*G(KK)*FR(KK)*F*QC)+BB
110 CONTINUE
AA=AE+EPS
AN=SQRT(.5*(AA+SQRT(AA**2+4.*(BB**2))))
AK=BB/AN
RETURN
END

```

APPENDIX F

PROGRAM LISTING AND INSTRUCTIONS FOR IBM SCIENTIFIC

SUBROUTINE - FMFP

(This material in this Appendix is a direct copy of an IBM Scientific Subroutine as it appears in IBM Manual GH20-0205-4 of System/360 Scientific Subroutine Package, Version III, Programmer's Manual.)

Extremum of Functions

Subroutines FMFP and DFMFP

These subroutines perform the calculation of an unconstrained minimum of a function of several variables using a method proposed by Davidson. The underlying method is described in the article by R. Fletcher and M.J.D. Powell, "A Rapidly Convergent Descent Method for Minimization", Computer Journal, vol. 6, iss. 2, 1963, pp. 163 - 168.

It is assumed that the function f of the n variables x_1, \dots, x_n (abbreviated as argument vector x) may be computed together with its gradient vector $g(x)$ for any point x . The generalized Taylor expansion for functions of several variables is

$$f(x+u) = f(x) + g(x) \cdot u + \frac{1}{2} u^T G(x) u + \text{higher terms}$$

where g is the gradient vector and G the matrix of second order partial derivatives. Vectors are assumed to be column vectors; u^T means transpose of vector u . It is assumed that in the neighborhood of the required minimum x_{\min} the function is approximated closely by the first three terms of its Taylor expansion, giving

$$f(x) = f(x_{\min}) + \frac{1}{2} (x - x_{\min})^T G(x_{\min}) (x - x_{\min})$$

since $g(x_{\min}) = 0$. Then the gradient is seen to be approximately $g(x) = G(x_{\min}) (x - x_{\min})$.

Assume now that the symmetric matrix G is positive definite. Then the following equation holds true:

$$x - x_{\min} = G^{-1}(x_{\min}) \cdot g(x)$$

which would allow x_{\min} to be calculated in one step if $G^{-1}(x_{\min})$ were available.

To approach $G^{-1}(x_{\min})$, a method of successive linear searches in G -conjugate directions is used. Starting with the identity matrix $G^{(0)} = I$, a sequence of symmetric matrices $G^{(i)}$ is generated which tends to G^{-1} . At the $(i+1)^{\text{st}}$ iteration step a linear search is made in direction $h^{(i)} = -G^{(i)} g^{(i)}$, where $g^{(i)}$ is an abbreviation for $g(x^{(i)})$. By means of the linear search the minimum of $y(t) = f(x^{(i)} + t \cdot h^{(i)})$ is determined, giving argument $x^{(i+1)} = x^{(i)} + t_i \cdot h^{(i)}$.

The argument of the minimum $x^{(i+1)}$ on the line through $x^{(i)}$ in direction $h^{(i)}$ is determined by the relation that scalar product $(g^{(i+1)}, h^{(i)}) = 0$.

$$\text{Now: } x^{(n)} = x^{(j)} + \sum_{i=j}^{n-1} t_i h^{(i)}$$

$$\text{and: } g^{(n)} = g^{(j)} + \sum_{i=j}^{n-1} t_i G h^{(i)}$$

Therefore:

$$\text{scalar product } (g^{(n)}, h^{(j)}) = \sum_{i=j+1}^{n-1} t_i (Gh^{(i)}, h^{(j)})$$

Suppose now that the vectors $h^{(0)}, h^{(1)}, \dots, h^{(n-1)}$ are G-conjugate, satisfying $(Gh^{(i)}, h^{(j)}) = 0$ for $i \neq j$. Then $(g^{(n)}, h^{(j)}) = 0$, and since $h^{(0)}, h^{(1)}, \dots, h^{(n-1)}$ form a basis, $g^{(n)} = 0$ and $x^{(n)} = x_{\min}$. This shows that the minimum is located at the n^{th} iteration for a quadratic function when using successive linear searches for G-conjugate directions.

For the generation of G-conjugate directions, start with $h^{(0)} = -g^{(0)}$ and calculate successive directions $h^{(l)}$ by means of $h^{(l)} = -G^{(l)} g^{(l)}$, where $G^{(l)}$ is modified to $G^{(l+1)}$ so that $h^{(l)}$ is an eigenvector of the matrix $G^{(l+1)}$ with eigenvalue 1. This ensures that $G^{(l)}$ approaches G^{-1} as $x^{(l)}$ approaches x_{\min} . An easy calculation shows:

$$G^{(l+1)} = G^{(l)} + \frac{dx \cdot dx^T}{dx^T \cdot dg} - \frac{G^{(l)} dg \cdot dg^T G^{(l)}}{dg^T G^{(l)} dg}$$

$$\text{with } dg = g^{(l+1)} - g^{(l)}$$

$$dx = x^{(l+1)} - x^{(l)}$$

where all vectors are regarded as column vectors, and superscript T means transpose of column vector--that is, row vector.

The strategy adopted for termination of the successive linear searches is as follows:

1. If the function value has not decreased in the last iteration step, the search for the minimum is terminated provided the gradient is already sufficiently small; otherwise, the next step is in the direction of steepest descent.

2. If the argument vector and the direction vector change by very small amounts, and at least n iterations are performed, the minimization is terminated again.

3. If the number of iterations exceeds an upper bound furnished by the user, further calculation is bypassed, and an error code is set to 1 indicating poor convergence.

4. If one of the successive linear searches indicates that no constrained minimum exists, further calculation is bypassed again, and the error code is set to 2 indicating that it is likely that no minimum exists.

The i^{th} term $G^{(i)}$ is reset to the identity matrix if there is indication that the current $G^{(i)}$ is not positive definite, or if the formula for $G^{(i+1)}$ breaks down due to zero divisors.

The linear search technique used in subroutines FMFP and DFMFP is as follows. For a given argument vector x and a vector h defining a direction through x , a local minimum of the function $y(t) = f(x+th)$ is determined. This means that a value t_m must be determined such that $y'(t_m) = 0$.

Given $y'(t) = \text{scalar product } (g(x+th), h)$, therefore $y(t)$ and $y'(t)$ may be calculated for any value of t , and:

$$y(0) = f(x) \text{ and } y'(0) = (g(x), h)$$

In case $y'(s_2) = 0$, t_m is set equal to s_2 and $x_m = x + s_2 \cdot h$ is used as argument of a constrained minimum on the line through x with direction h . In the second and third case a minimum lies between the points $x_1 = x + s_1 \cdot h$ and $x_2 = x + s_2 \cdot h$; that is, t_m must be in the interval (s_1, s_2) .

The argument of the minimum is obtained by means of cubic interpolation using the function and derivative values at the points x_1, x_2 . Let $x_3 = x + s_3 \cdot h$ be the argument of the minimum of the third degree interpolation polynomial. Then:

$$s_3 = s_2 - \alpha(s_2 - s_1) = s_1 + (\alpha - 1)(s_1 - s_2)$$

$$\text{with: } \alpha = \frac{y'(s_2) + w - z}{y'(s_2) - y'(s_1) + 2w}$$

$$\text{and: } z = 3 \frac{y(s_2) - y(s_1)}{s_2 - s_1} + y'(s_1) + y'(s_2)$$

$$w = \sqrt{[z^2 - y'(s_1) \cdot y'(s_2)]}$$

If $f(x_3) \leq f(x_1)$ and $f(x_3) \leq f(x_2)$, x_m is set equal to x_3 and used as argument of the wanted minimum along the given line. Otherwise the interval (x_1, x_2) is reduced by replacing x_1 by x_3 if $f(x_3) \leq f(x_1)$ and $[g(x_1), h] < 0$, and by replacing x_2 by x_3 in all other cases. Then the interpolation process is repeated for this new reduced interval.

Mathematics--Extremum of
Functions

1	C		FMEP	10
2	C	FMEP	20
3	C		FMEP	30
4	C	SUBROUTINE FMEP	FMEP	40
5	C		FMEP	50
6	C	PURPOSE	FMEP	60
7	C	TO FIND A LOCAL MINIMUM OF A FUNCTION OF SEVERAL VARIABLES	FMEP	70
8	C	BY THE METHOD OF FLETCHER AND POWELL	FMEP	80
9	C		FMEP	90
10	C	USAGE	FMEP	100
11	C	CALL FMEP(FUNCT,N,X,F,G,EST,EPS,LIMIT,IER,H)	FMEP	110
12	C		FMEP	120
13	C	DESCRIPTION OF PARAMETERS	FMEP	130
14	C	FUNCT - USER-WRITTEN SUBROUTINE CONCERNING THE FUNCTION TO	FMEP	140
15	C	BE MINIMIZED. IT MUST BE OF THE FORM	FMEP	150
16	C	SUBROUTINE FUNCT(N,ARG,VAL,GRAD)	FMEP	160
17	C	AND MUST SERVE THE FOLLOWING PURPOSE	FMEP	170
18	C	FOR EACH N-DIMENSIONAL ARGUMENT VECTOR ARG,	FMEP	180
19	C	FUNCTION VALUE AND GRADIENT VECTOR MUST BE COMPUTED	FMEP	190
20	C	AND, ON RETURN, STORED IN VAL AND GRAD RESPECTIVELY	FMEP	200
21	C	N - NUMBER OF VARIABLES	FMEP	210
22	C	X - VECTOR OF DIMENSION N CONTAINING THE INITIAL	FMEP	220
23	C	ARGUMENT WHERE THE ITERATION STARTS. ON RETURN,	FMEP	230
24	C	X HOLDS THE ARGUMENT CORRESPONDING TO THE	FMEP	240
25	C	COMPUTED MINIMUM FUNCTION VALUE	FMEP	250
26	C	F - SINGLE VARIABLE CONTAINING THE MINIMUM FUNCTION	FMEP	260
27	C	VALUE ON RETURN, I.E. $F=F(X)$.	FMEP	270
28	C	G - VECTOR OF DIMENSION N CONTAINING THE GRADIENT	FMEP	280
29	C	VECTOR CORRESPONDING TO THE MINIMUM ON RETURN,	FMEP	290
30	C	I.E. $G=G(X)$.	FMEP	300
31	C	EST - IS AN ESTIMATE OF THE MINIMUM FUNCTION VALUE.	FMEP	310
32	C	EPS - TESTVALUE REPRESENTING THE EXPECTED ABSOLUTE ERROR.	FMEP	320
33	C	A REASONABLE CHOICE IS $10^{-(6)}$, I.E.	FMEP	330
34	C	SOMEWHAT GREATER THAN $10^{-(D)}$, WHERE D IS THE	FMEP	340
35	C	NUMBER OF SIGNIFICANT DIGITS IN FLOATING POINT	FMEP	350
36	C	REPRESENTATION.	FMEP	360
37	C	LIMIT - MAXIMUM NUMBER OF ITERATIONS.	FMEP	370
38	C	IER - ERROR PARAMETER	FMEP	380
39	C	IER = 0 MEANS CONVERGENCE WAS OBTAINED.	FMEP	390
40	C	IER = 1 MEANS NO CONVERGENCE IN LIMIT ITERATIONS	FMEP	400
41	C	IER = -1 MEANS ERRORS IN GRADIENT CALCULATION	FMEP	410
42	C	IER = 2 MEANS LINEAR SEARCH TECHNIQUE INDICATES	FMEP	420
43	C	IT IS LIKELY THAT THERE EXISTS NO MINIMUM.	FMEP	430
44	C	H - WORKING STORAGE OF DIMENSION $N*(N+7)/2$.	FMEP	440
45	C		FMEP	450
46	C	REMARKS	FMEP	460
47	C	I) THE SUBROUTINE NAME REPLACING THE DUMMY ARGUMENT FUNCT	FMEP	470
48	C	MUST BE DECLARED AS EXTERNAL IN THE CALLING PROGRAM.	FMEP	480
49	C	II) IER IS SET TO 2 IF, STEPPING IN ONE OF THE COMPUTED	FMEP	490
50	C	DIRECTIONS, THE FUNCTION WILL NEVER INCREASE WITHIN	FMEP	500
51	C	A TOLERABLE RANGE OF ARGUMENT.	FMEP	510
52	C	IER = 2 MAY OCCUR ALSO IF THE INTERVAL WHERE F	FMEP	520
53	C	INCREASES IS SMALL AND THE INITIAL ARGUMENT WAS	FMEP	530
54	C	RELATIVELY FAR AWAY FROM THE MINIMUM SUCH THAT THE	FMEP	540
55	C	MINIMUM WAS OVERLEAPED. THIS IS DUE TO THE SEARCH	FMEP	550
56	C	TECHNIQUE WHICH DOUBLES THE STEPSIZE UNTIL A POINT	FMEP	560
57	C	IS FOUND WHERE THE FUNCTION INCREASES.	FMEP	570
58	C		FMEP	580
59	C	SUBROUTINES AND FUNCTION SUBPROGRAMS REQUIRED	FMEP	590
60	C	FUNCT	FMEP	600

61	C		FMFP 610
62	C	METHOD	FMFP 620
63	C	THE METHOD IS DESCRIBED IN THE FOLLOWING ARTICLE	FMFP 630
64	C	H. FLETCHER AND H.J.D. POWELL, A RAPID DESCENT METHOD FOR	FMFP 640
65	C	MINIMIZATION,	FMFP 650
66	C	COMPUTER JOURNAL VOL.6, ISS. 2, 1963, PP.163-168.	FMFP 660
67	C		FMFP 670
68	C	FMFP 680
69	C		FMFP 690
70		SUBROUTINE FMFP(FUNCT,N,X,F,G,EST,EPS,LIMIT,IER,H)	FMFP 700
71	C		FMFP 710
72	C	DIMENSIONED DUMMY VARIABLES	FMFP 720
73		DTMENSION H(1),X(1),G(1)	FMFP 730
74	C		FMFP 740
75	C	COMPUTE FUNCTION VALUE AND GRADIENT VECTOR FOR INITIAL ARGUMENT	FMFP 750
76		CALL FUNCT(N,X,F,G)	FMFP 760
77	C		FMFP 770
78	C	RESET ITERATION COUNTER AND GENERATE IDENTITY MATRIX	FMFP 780
79		IER=0	FMFP 790
80		KOUNT=0	FMFP 800
81		N2=N+N	FMFP 810
82		N3=N2+N	FMFP 820
83		N31=N3+1	FMFP 830
84		1 K=N31	FMFP 840
85		DO 4 J=1,N	FMFP 850
86		H(K)=1.	FMFP 860
87		N1=N-1	FMFP 870
88		IF(NJ)5,5,2	FMFP 880
89		2 DO 3 L=1,NJ	FMFP 890
90		KL=K+L	FMFP 900
91		3 H(KL)=0.	FMFP 910
92		4 K=KL+1	FMFP 920
93	C		FMFP 930
94	C	START ITERATION LOOP	FMFP 940
95		5 KOUNT=KOUNT +1	FMFP 950
96	C		FMFP 960
97	C	SAVE FUNCTION VALUE, ARGUMENT VECTOR AND GRADIENT VECTOR	FMFP 970
98		OLDF=F	FMFP 980
99		DO 9 J=1,N	FMFP 990
100		K=N+J	FMFP1000
101		H(K)=G(J)	FMFP1010
102		K=N+N	FMFP1020
103		H(K)=X(J)	FMFP1030
104	C		FMFP1040
105	C	DETERMINE DIRECTION VECTOR H	FMFP1050
106		K=N+3	FMFP1060
107		T=0.	FMFP1070
108		DO 8 L=1,N	FMFP1080
109		T=T-G(L)*H(K)	FMFP1090
110		IF(L=J)6,7,7	FMFP1100
111		6 K=N+N-L	FMFP1110
112		GO TO 8	FMFP1120
113		7 K=K+1	FMFP1130
114		8 CONTINUE	FMFP1140
115		9 H(J)=T	FMFP1150
116	C		FMFP1160
117	C	CHECK WHETHER FUNCTION WILL DECREASE STEPPING ALONG H.	FMFP1170
118		DY=0.	FMFP1180
119		HNRN=0.	FMFP1190
120		GWRN=0.	FMFP1200

121	C		FMEP1210
122	C	CALCULATE DIRECTIONAL DERIVATIVE AND TEST VALUES FOR DIRECTION	FMEP1220
123	C	VECTOR H AND GRADIENT VECTOR G.	FMEP1230
124		DO 10 J=1,N	FMEP1240
125		HNRH=HNRH+ARS(H(J))	FMEP1250
126		GHRH=GHRH+ARS(G(J))	FMEP1260
127		10 DY=DY+H(J)*G(J)	FMEP1270
128	C		FMEP1280
129	C	REPEAT SEARCH IN DIRECTION OF STEEPEST DESCENT IF DIRECTIONAL	FMEP1290
130	C	DERIVATIVE APPEARS TO BE POSITIVE OR ZERO.	FMEP1300
131		IF(DY)11,51,51	FMEP1310
132	C		FMEP1320
133	C	REPEAT SEARCH IN DIRECTION OF STEEPEST DESCENT IF DIRECTION	FMEP1330
134	C	VECTOR H IS SMALL COMPARED TO GRADIENT VECTOR G.	FMEP1340
135		11 IF(HNRH/GHRH=EPS)51,51,12	FMEP1350
136	C		FMEP1360
137	C	SEARCH MINIMUM ALONG DIRECTION H	FMEP1370
138	C		FMEP1380
139	C	SEARCH ALONG H FOR POSITIVE DIRECTIONAL DERIVATIVE	FMEP1390
140		12 FY=F	FMEP1400
141		ALFA=2.*(EST-F)/DY	FMEP1410
142		AMBDA=1.	FMEP1420
143	C		FMEP1430
144	C	USE ESTIMATE FOR STEPSIZE ONLY IF IT IS POSITIVE AND LESS THAN	FMEP1440
145	C	1, OTHERWISE TAKE 1, AS STEPSIZE	FMEP1450
146		IF(ALFA)15,15,13	FMEP1460
147		13 IF(ALFA=AMBDA)14,15,15	FMEP1470
148		14 AMBDA=ALFA	FMEP1480
149		15 ALFA=0.	FMEP1490
150	C		FMEP1500
151	C	SAVE FUNCTION AND DERIVATIVE VALUES FOR OLD ARGUMENT	FMEP1510
152		16 FX=FY	FMEP1520
153		DY=DY	FMEP1530
154	C		FMEP1540
155	C	STEP ARGUMENT ALONG H	FMEP1550
156		DO 17 I=1,N	FMEP1560
157		17 X(I)=X(I)+AMBDA*H(I)	FMEP1570
158	C		FMEP1580
159	C	COMPUTE FUNCTION VALUE AND GRADIENT FOR NEW ARGUMENT	FMEP1590
160		CALL FUNCT(N,X,F,G)	FMEP1600
161		FY=F	FMEP1610
162	C		FMEP1620
163	C	COMPUTE DIRECTIONAL DERIVATIVE DY FOR NEW ARGUMENT. TERMINATE	FMEP1630
164	C	SEARCH, IF DY IS POSITIVE. IF DY IS ZERO THE MINIMUM IS FOUND	FMEP1640
165		DY=0.	FMEP1650
166		DO 18 I=1,N	FMEP1660
167		18 DY=DY+G(I)*H(I)	FMEP1670
168		IF(DY)19,36,22	FMEP1680
169	C		FMEP1690
170	C	TERMINATE SEARCH ALSO IF THE FUNCTION VALUE INDICATES THAT	FMEP1700
171	C	A MINIMUM HAS BEEN PASSED	FMEP1710
172		19 IF(FY-FX)20,22,22	FMEP1720
173	C		FMEP1730
174	C	REPEAT SEARCH AND DOUBLE STEPSIZE FOR FURTHER SEARCHES	FMEP1740
175		20 AMBDA=AMBDA*ALFA	FMEP1750
176		ALFA=AMRDA	FMEP1760
177	C	END OF SEARCH LOOP	FMEP1770
178	C		FMEP1780
179	C	TERMINATE IF THE CHANGE IN ARGUMENT GETS VERY LARGE	FMEP1790
180		IF(HNRH*AMBDA=1.E10)16,16,21	FMEP1800

191	C			FMP1810
192	C		LINEAR SEARCH TECHNIQUE INDICATES THAT NO MINIMUM EXISTS	FMP1820
193		21	IER=2	FMP1830
194			RETURN	FMP1840
195	C			FMP1850
196	C		INTERPOLATE CURVICALLY IN THE INTERVAL DEFINED BY THE SEARCH	FMP1860
197	C		ABOVE AND COMPUTE THE ARGUMENT X FOR WHICH THE INTERPOLATION	FMP1870
198	C		POLYNOMIAL IS MINIMIZED	FMP1880
199		22	T=0.	FMP1890
200		23	IF (AMRDA) 24, 36, 24	FMP1900
201		24	Z=3.*(FY-FY)/AMRDA+DX+DY	FMP1910
202			ALFA=AMAX1(ABS(Z),ARS(DX),ABS(DY))	FMP1920
203			DALFA=Z/ALFA	FMP1930
204			DALFA=DALFA+DALFA-DX/ALFA+DY/ALFA	FMP1940
205			IF (DALFA) 51, 25, 25	FMP1950
206		25	H=ALFA*SQRT(DALFA)	FMP1960
207			ALFA=DY-DX+H+H	
208			IF (ALFA) 250, 251, 250	
209		250	ALFA=(DY-Z+H)/ALFA	
210			GO TO 252	
211		251	ALFA=(Z+DY-H)/(Z+DX+Z+DY)	
212		252	ALFA=ALFA*AMBDA	
213			DO 26 I=1, N	FMP1980
214		26	X(I)=X(I)+(T-ALFA)*H(I)	FMP1990
215	C			FMP2000
216	C		TERMINATE, IF THE VALUE OF THE ACTUAL FUNCTION AT X IS LESS	FMP2010
217	C		THAN THE FUNCTION VALUES AT THE INTERVAL ENDS, OTHERWISE REDUCE	FMP2020
218	C		THE INTERVAL BY CHOOSING ONE END-POINT EQUAL TO X AND REPEAT	FMP2030
219	C		THE INTERPOLATION, WHICH END-POINT IS CHOSEN DEPENDS ON THE	FMP2040
220	C		VALUE OF THE FUNCTION AND ITS GRADIENT AT X	FMP2050
221	C			FMP2060
222			CALL FUNCT(N,X,F,G)	FMP2070
223			IF (F-FX) 27, 27, 28	FMP2080
224		27	IF (F-FY) 36, 36, 28	FMP2090
225		28	DALFA=0.	FMP2100
226			DO 29 I=1, N	FMP2110
227		29	DALFA=DALFA+G(I)*H(I)	FMP2120
228			IF (DALFA) 30, 33, 33	FMP2130
229		30	IF (F-FX) 32, 31, 33	FMP2140
230		31	IF (DX-DALFA) 32, 36, 32	FMP2150
231		32	FX=F	FMP2160
232			DX=DALFA	FMP2170
233			T=ALFA	FMP2180
234			AMBDA=ALFA	FMP2190
235			GO TO 23	FMP2200
236		33	IF (FY-F) 35, 34, 35	FMP2210
237		34	IF (DY-DALFA) 35, 36, 35	FMP2220
238		35	FY=F	FMP2230
239			DY=DALFA	FMP2240
240			AMBDA=AMBDA-ALFA	FMP2250
241			GO TO 22	FMP2260
242	C			FMP2270
243	C		TERMINATE, IF FUNCTION HAS NOT DECREASED DURING LAST ITERATION	
244		36	IF (OLDF-F*EPS) 51, 50, 38	
245	C			
246	C		COMPUTE DIFFERENCE VECTORS OF ARGUMENT AND GRADIENT FROM	
247	C		TWO CONSECUTIVE ITERATIONS	
248		38	DO 37 J=1, N	
249			K=N+J	
250			H(K)=G(J)-H(K)	

241		K=N+K	
242		37 H(K)=X(J)-H(K)	
243	C		FMFP2380
244	C	TEST LENGTH OF ARGUMENT DIFFERENCE VECTOR AND DIRECTION VECTOR	FMFP2390
245	C	IF AT LEAST N ITERATIONS HAVE BEEN EXECUTED, TERMINATE, IF	FMFP2400
246	C	BOTH ARE LESS THAN EPS	FMFP2410
247		IFR=0	
248		IF(KOUNT-N)42,39,39	FMFP2430
249	39	T=0.	FMFP2440
250		Z=0.	FMFP2450
251		DO 40 J=1,N	FMFP2460
252		K=N+J	FMFP2470
253		M=H(K)	FMFP2480
254		K=K+N	FMFP2490
255		T=T+ABS(H(K))	FMFP2500
256	40	Z=Z+M*H(K)	FMFP2510
257		IF(MNRM=EPS)41,41,42	FMFP2520
258	41	IF(T-FPS)56,56,42	FMFP2530
259	C		FMFP2540
260	C	TERMINATE, IF NUMBER OF ITERATIONS WOULD EXCEED LIMIT	FMFP2550
261	42	IF(KOUNT-LIMIT)43,50,50	FMFP2560
262	C		FMFP2570
263	C	PREPARE UPDATING OF MATRIX H	FMFP2580
264	43	ALFA=0.	FMFP2590
265		DO 47 J=1,N	FMFP2600
266		K=J+N3	FMFP2610
267		M=0.	FMFP2620
268		DO 46 L=1,N	FMFP2630
269		KL=N+L	FMFP2640
270		M=M+H(KL)*H(K)	FMFP2650
271		IF(L=J)44,45,45	FMFP2660
272	44	K=K+N-L	FMFP2670
273		GO TO 46	FMFP2680
274	45	K=K+1	FMFP2690
275	46	CONTINUE	FMFP2700
276		K=N+J	FMFP2710
277		ALFA=ALFA+M*H(K)	FMFP2720
278	47	H(J)=M	FMFP2730
279	C		FMFP2740
280	C	REPEAT SEARCH IN DIRECTION OF STEEPEST DESCENT IF RESULTS	FMFP2750
281	C	ARE NOT SATISFACTORY	FMFP2760
282		IF(Z*ALFA)48,1,48	FMFP2770
283	C		FMFP2780
284	C	UPDATE MATRIX H	FMFP2790
285	48	K=N31	FMFP2800
286		DO 49 L=1,N	FMFP2810
287		KL=N2+L	FMFP2820
288		DO 49 J=L,N	FMFP2830
289		NJ=N2+J	FMFP2840
290		H(K)=H(K)+H(KL)*H(NJ)/Z-H(L)*H(J)/ALFA	FMFP2850
291	49	K=K+1	FMFP2860
292		GO TO 5	FMFP2870
293	C	END OF ITERATION LOOP	FMFP2880
294	C		FMFP2890
295	C	NO CONVERGENCE AFTER LIMIT ITERATIONS	FMFP2900
296	50	IFR=1	FMFP2910
297		RETURN	FMFP2920
298	C		FMFP2930
299	C	RESTORE OLD VALUES OF FUNCTION AND ARGUMENTS	FMFP2940
300	51	DO 52 J=1,N	FMFP2950

301		K=N2+J	FMFP2960
302		52 X(J)=H(K)	FMFP2970
303		CALL FUNCT(N,X,F,G)	FMFP2980
304	C		FMFP2990
305	C	REPEAT SEARCH IN DIRECTION OF STEEPEST DESCENT IF DERIVATIVE	FMFP3000
306	C	FAILS TO BE SUFFICIENTLY SMALL	FMFP3010
307		IF(GNRN-EP8)55,55,53	FMFP3020
308	C		FMFP3030
309	C	TEST FOR REPEATED FAILURE OF ITERATION	FMFP3040
310		53 IF(IER)56,54,54	FMFP3050
311		54 IER=-1	FMFP3060
312		GO TO 1	FMFP3070
313		55 IFR=0	FMFP3080
314		56 RETURN	FMFP3090
315		END	FMFP3100

END OF FILE